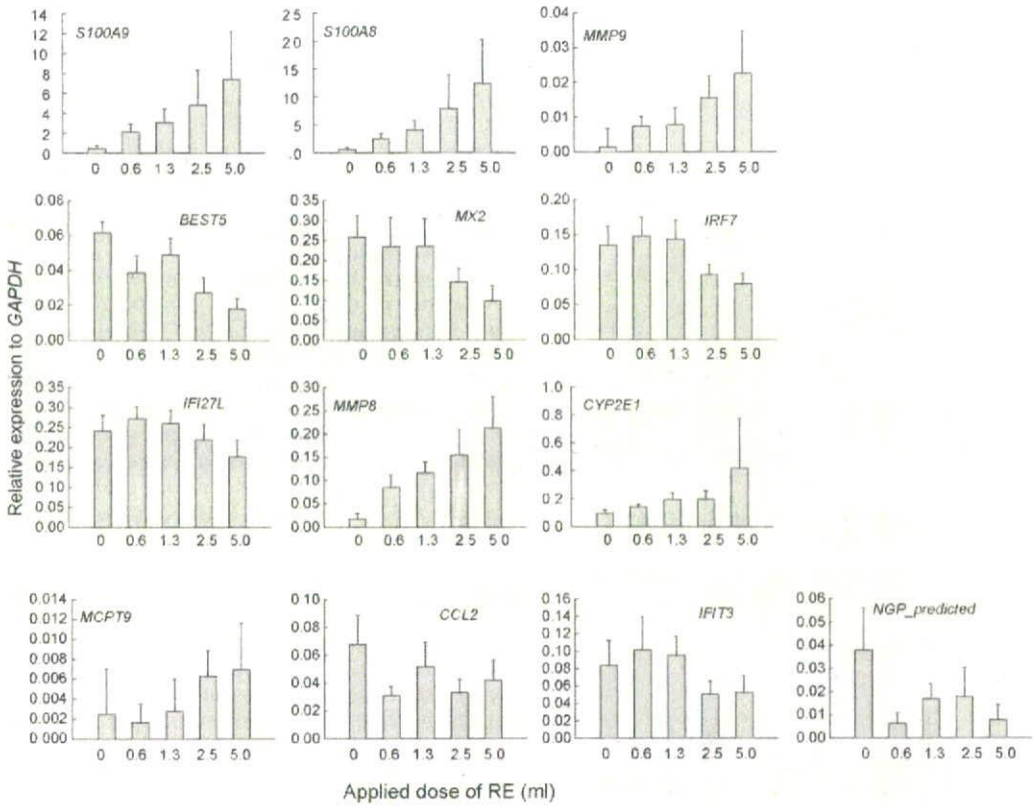

Fig. 7. Toxicity-related biomarkers of pertussis vaccine. SA- and various doses of RE-treated lung lysates were analyzed with QuantiGene Plex assay. Three to five animals for each sample were assayed by QuantiGene Plex in two experiments and shown as the mean expression ± S.D.

liver is thought to be one of the most appropriate organs to analyze the biological alteration with vaccine toxicity, because it is the major organ that metabolizes toxic agents. Moreover, many studies regarding pharmaceutical toxicity analysis in the liver using DNA microarray are ongoing [11]. In our previous study, we clarified the pertussis toxin-related genes by analyzing the expression profiles for RE-treated liver [12]. In this study, we performed clustering analysis for the vaccine or toxin treated tissues. However, the expression level of toxicity-related genes showed various in liver (Fig. 4A), kidney (Fig. 4B), and brain (Fig. 4C) depending on the sample treated animals. On the other hand, the lung genes which were extracted by DNA microarray classified the clusters sharply. Only sample #202 in Fig. 3 was miss-categorized in the wrong cluster. This sample was subsequently confirmed to be a technical accident. Besides sample #202, the clustering results of the lung are quite neat. From these results, we could recognize three important points regarding the lung samples. First, the data from two independents closely correspond to each other, meaning that the expression pattern in the lung is repeatable. Second, the clustering analysis showed clear categorization, meaning that the expression pattern of clustered PT- and RE-treated samples were strictly separated from that of SA- and PV-treated samples. Third, clear categorization was seen from day 1, meaning that the gene expression data was sensitive to detect vaccine effects. Furthermore, the clustering data from the lung was revealed to be reproducible. These results from the lung also demonstrated an interesting opinion that lung might be the most suitable organ for detecting the toxicity contained in pertussis vaccine using comprehensive microarray analysis.

Recently, McGuirk et al. elucidated the mechanisms involved in immune reactions between *B. pertussis* and pertussis vaccine in the lung, and a dramatic influx of neutrophils was observed in the lungs following *B. pertussis* infection of non-immunized mice [13]. Moreover, the inflammatory response was suppressed in the lungs of mice immunized with Th1-inducing killed-whole bacteria vaccine or Th2-inducing subunit vaccine [14]. These findings suggest that the functional responses and phenotype of local pulmonary T cells are generated by respiratory infection with *B. pertussis*, and the lung is a key organ, which functions as a protector for inflammatory responses. Other organs such as the kidney and brain did not show any clear clustering patterns by microarray analysis, meaning that of the four organs tested, the lung should be a feasible organ to analyze the expression pattern of toxicity-related genes in the case of pertussis vaccines.

Focused on the genes, which showed dramatically altered expression pattern in PT-treated samples compared with SA-treated ones in the lung (expression ratios over 0.75 in $\log_2$ scale on average ($P < 0.01$)), at day 1 post-administration, 25 transcripts were extracted to distinguish the individual samples. As shown in Figs. 3 and 4, RE- and PT-treated samples were sharply distinguished from SA- and PV-treated samples in lung, although brain, kidney, and liver samples did not have a similar contrast. In these 25 transcripts, the expression of 13 genes was correlated between the microarray data and Real-Time PCR data. These 13 "signatures" should be the predictive biomarkers of toxicant effect included in the vaccine. Using these signatures, we tried to develop more sensitive and more scientifically well-grounded methods for the quality control of vaccines.

Table 3
"Genetic signatures" for pertussis vaccine toxicity

Accession No.	Symbol	Category	Description	SA	PV	PT	RE
NM_053587	*S100a9*	Inflammation	A calcium binding protein that may be associated with acute inflammatory processes, coupled with S100a8	−1.40 ± 0.69	−0.98 ± 0.37	0.58 ± 0.40	2.84 ± 0.41
NM_019323	*Mcpt9*	Inflammation	A serine protease expressed in mast cells, but the precise function has not yet determined	−2.72 ± 0.30	−2.48 ± 0.27	0.57 ± 0.35	−1.58 ± 0.25
NM_053822	*S100a8*	Inflammation	May play a role in inflammatory responses such as cell motility, coupled with S100a9	−2.68 ± 0.67	−2.22 ± 0.46	−0.56 ± 0.54	2.14 ± 0.45
NM_031055	Mmp9	Peptidoglycan metabolism	Metalloproteinase involved in extracellular matrix remodeling, bone resorption, and immune responses	−2.21 ± 0.40	−2.25 ± 0.41	−1.30 ± 0.34	−0.35 ± 0.19
Y07704	*Best5*	Ossification	Induced by IFN and involved in bone formation	−0.22 ± 0.36	−0.36 ± 0.35	−1.03 ± 012	−1.37 ± 0.10
NM_017028	*Mx2*	Immune response	Involved in inhibiting vesicular stomatitis virus, but not an anti-influenza molecule	0.77 ± 0.30	0.72 ± 0.27	−0.33 ± 0.14	0.05 ± 0.25
XM_215121	*Irf7*	-	Unknown	0.81 ± 0.11	0.82 ± 0.16	0.04 ± 0.25	0.60 ± 0.21
NM_130743	*Ifi27l*	Immune response	Induced by steroid hormone, IFN and LPS in endometrium at implantation, dendric cells and macrophases	0.86 ± 0.35	0.36 ± 0.37	−0.02 ± 0.15	0.40 ± 0.23
NM_031530	*Ccl2*	Inflammation	A ligand for CCR2 that acts as a chemoattractant of monocytes	−0.09 ± 0.18	0.01 ± 0.10	1.12 ± 0.58	0.54 ± 0.39
XM_220059	Ifit3	Immune response	May induced by IFN or virus infection	2.42 ± 0.13	2.35 ± 0.48	1.20 ± 0.66	2.55 ± 0.39
NM_022221	*Mmp8*	Peptidoglycan metabolism	May play a role in appositional bone formation and regulation of the extracellular matrix	−0.23 ± 0.67	0.32 ± 0.24	2.04 ± 0.51	3.23 ± 0.45
J02627	*Cyp2e1*	Xenobiotic metabolism	Protects hepatocytes from stress-induced cell death	−4.03 ± 0.21	−3.93 ± 0.23	−3.25 ± 0.21	−0.71 ± 0.52
XM_236646	*Ngp_predicted*	-	Neutrophilic granule protein (predicted)	−3.38 ± 0.61	−3.04 ± 0.50	−1.33 ± 0.48	−3.04 ± 0.45

Cyanine 5-labeled lung RNA and Cyanine 3-labeled rat common reference RNA were competitively hybridized to microarrays. Hybridizaiton signals were processed into primary expression ratios ([Cyanine 5-intensity obtained from each sample]/[Cyanine 3-intensity obtained from common reference RNA]), and normalized (primary expression ratios). The primary expression ratios were converted into $\log_2$ values ($\log_2$ Cyanine 5-intensity/Cyanine 3-intensity) as described in Section 2. $\log_2$ values for each sample were taken an average and calculated S.D.

Of these 13 genes, five independent genes were universally selected throughout the testing periods, such as *S100A9* (NM_053587), *MCPT9* (NM_019323) *S100A8* (NM_053822), *CCL2* (M57441), and *MMP8* (NM_022221). Consistent with studies by McGuirk and colleagues, the five genes obtained from our microarray analysis are mainly associated with inflammatory or anti-inflammatory responses. S100A8 and S100A9 belong to the S100 protein family, which is characterized by the presence of two EF-hand type calcium-binding motifs [15]. They are mainly produced by phagocytes and form homo- and heterodimers in a calcium-dependent manner, causing neutrophil infiltration. Overexpression of these proteins were observed at local sites of inflammation, and elevated serum levels have been found along with a number of inflammatory disorders [16,17]. MCPT9 was cloned from a mucosal mast cell cDNA library in 1997 [18,19]. The expression of MCPT9 in connective tissue mast cells may be relatively low, but it is one of the major proteases in mucosal mast cell granules. It has a putative proteinase activity and apparently lacks tryptase, but the precise function of MCPT9 has not been elucidated. CCL2 is a member of the CC chemokine family involved in leukocyte physiology and trafficking. CCL2 mediates monocyte recruitment and entry into vessel walls. Overexpression of CCL2 led to atherosclerosis [20], and observed during the acute phase of several inflammatory disorders in human [20,21]. In a clinical study, the CCL2 level in plasma is accumulated along with lipid abnormalities [22]. MMP8 is one of the interstitial collagenases of the MMP family of extracellular and cell-surface associated, highly conserved zinc-dependent endopeptidases. MMP8 is mainly produced by neutrophils, and its collagenase activity is considered to correlate with neutrophil infiltration. In contrast, recent data from *MMP8-/-* mice in an asthma model showed increased neutrophilic and eosinophilic infiltration in the airway walls, indicating anti-inflammatory roles of MMP8 [23,24]. By accumulating the microarray-based information regarding vaccine treated samples, the mechanisms of vaccine toxicity will be elucidated genetically.

Although we identified 13 toxicity-related genes from the microarray analysis, it took a lot of effort to quantify all the genes by Real-Time PCR one by one. In order to quantify these genes in a convenient way, QuantiGene Plex assay was applied. QuantiGene Plex assay can deal with 13 genes in one reaction well. Furthermore, we can use the tissue lysate sample for the reactions instead of their purified RNAs, meaning that the assay avoids variation or errors resulting from extraction and amplification. Data for all 13 genes from QuantiGene Plex assay were closely correlated with the data from Real-Time PCR, and the quality was validated, as shown in Fig. 6. In Fig. 7, *S100A9*, *S100A8*, *MMP9*, *BEST5*, *MX2*, *IRF7*, *IFI27L*, *MMP8*, and *CYP2E1* were found to be suitable markers for RE vaccine toxicity. Furthermore, we confirmed that RE vaccine toxicity was measurable by means of the specific expression level of these nine genes in the lung lysate. The QuantiGene Plex assay has the advantages of the handling-convenience and the data-accuracy. For the new control test for vaccine toxicity, this assay will be one of the expecting candidates.

Some vaccines have been highly purified and their components crystallized, and their structures have been evaluated at the molecular level. However, we are still required to perform safety tests before the releasing the vaccine lots. Using the animal safety tests, we could detect severe weight loss, which was highly related to RE-treatment (Fig. 1), but the level of weight loss is not consistent between the tested animals. Histological studies with the treated-animals did not show any abnormal appearance in RE or PT treated lung sections (Fig. 3E). Conventional animal tests should be improved in many points. Nowadays, the four Rs, Replacement,

Reduction, Refinement, and Responsibility of animal experiments are advocated. To reduce the number of animals for safety tests and to refine the test's sensitivity, we are required to use the new vaccine evaluation system. Since the quantification of array-precipitated gene in this study is reproducible and objective, we think that it is possible to reduce the number of animals to confirm the safety of vaccines.

In this study, we focused on the pertussis vaccine. In the future, for the evaluation of all kinds of vaccines, this microarray analysis will play an important role as the new safety control test, especially for checking the toxin reactive transcripts. For another purpose of development of this vaccine-evaluation assay, we would utilize this for developing new vaccines. Nowadays, we are on the verge of a pandemic of high pathogenic influenza; therefore, new effective vaccines are urgently required. However, the evaluation of vaccine safety involves a long period of time to conduct tests and seek regulatory approval. In order to speed up vaccine production, we hope this assay would provide us with a strong tool for quicker development of new and effective vaccines.

References

[1] Sato H, Sato Y. *Bordetella pertussis* infection in mice: correlation of specific antibodies against two antigens, pertussis toxin, and filamentous hemagglutinin with mouse protectivity in an intracerebral or aerosol challenge system. Infect Immun 1984;46(November (2)):415–21.

[2] Atlanta G. Epidemiology and prevention of vaccine-preventable diseases. 8 ed. CDC, National Immunizing Program; 2000.

[3] Horiuchi Y, Takahashi M, Konda T, Ochiai M, Yamamoto A, Kataoka M, et al. Quality control of diphtheria tetanus acellular pertussis combined (DTaP) vaccines in Japan. Jpn J Infect Dis 2001;54(October (5)):167–80.

[4] Kurokawa M. Toxicity and toxicity testing of pertussis vaccine. Jpn J Med Sci Biol 1984;37(April (2)):41–81.

[5] Hamadeh HK, Bushel PR, Jayadev S, Martin K, DiSorbo O, Sieber S, et al. Gene expression analysis reveals chemical-specific profiles. Toxicol Sci 2002;67(June (2)):219–31.

[6] Ejiri N, Katayama K, Kiyosawa N, Baba Y, Doi K. Microarray analysis on Phase II drug metabolizing enzymes expression in pregnant rats after treatment with pregnenolone-16alpha-carbonitrile or phenobarbital. Exp Mol Pathol 2005;79(December (3)):272–7.

[7] Ministry of Health Welfare, J.G. The minimum requirements of biological products of Japan 1986. Tokyo: Ministry of Health and Welfare; 1986.

[8] Kobayashi S, Ito E, Honma R, Nojima Y, Shibuya M, Watanabe S, et al. Dynamic regulation of gene expression by the Flt-1 kinase and Matrigel in endothelial tubulogenesis. Genomics 2004;84(July (1)):185–92.

[9] Ito E, Honma R, Imai J, Azuma S, Kanno T, Mori S, et al. A tetraspanin-family protein, T-cell acute lymphoblastic leukemia-associated antigen 1, is induced by the Ewing's sarcoma-Wilms' tumor 1 fusion protein of desmoplastic small round-cell tumor. Am J Pathol 2003;163(December (6)):2165–72.

[10] Canales RD, Luo Y, Willey JC, Austermiller B, Barbacioru CC, Boysen C, et al. Evaluation of DNA microarray results with quantitative gene expression platforms. Nat Biotechnol 2006;24(September (9)):1115–22.

[11] Shipkova M, Spielbauer B, Voland A, Grone HJ, Armstrong VW, Oellerich M, et al. cDNA microarray analysis reveals new candidate genes possibly linked to side effects under mycophenolate mofetil therapy. Transplantation 2004;78(October (8)):1145–52.

[12] Hamaguchi I, Imai J, Momose H, Kawamura M, Mizukami T, Kato H, et al. Two vaccine toxicity-related genes Agp and Hpx could prove useful for pertussis vaccine safety control. Vaccine 2007;25(April (17)):3355–64.

[13] McGuirk P, Mahon BP, Griffin F, Mills KH. Compartmentalization of T cell responses following respiratory infection with *Bordetella pertussis*: hyporesponsiveness of lung T cells is associated with modulated expression of the co-stimulatory molecule CD28. Eur J Immunol 1998;28(January (1)):153–63.

[14] McGuirk P, Mills KH. A regulatory role for interleukin 4 in differential inflammatory responses in the lung following infection of mice primed with Th1- or Th2-inducing pertussis vaccines. Infect Immun 2000;68(March (3)):1383–90.

[15] Roth J, Vogl T, Sorg C, Sunderkotter C. Phagocyte-specific S100 proteins: a novel group of proinflammatory molecules. Trends Immunol 2003;24(April (4)):155–8.

[16] Bozinovski S, Cross M, Vlahos R, Jones JE, Hsuu K, Tessier PA, et al. S100A8 chemotactic protein is abundantly increased, but only a minor contributor to LPS-induced, steroid resistant neutrophilic lung inflammation in vivo. J Proteome Res 2005;4(January–February (1)):136–45.

[17] Yui S, Nakatani Y, Mikami M, Calprotectin. (S100A8/S100A9), an inflammatory protein complex from neutrophils with a broad apoptosis-inducing activity. Biol Pharm Bull 2003;26(June (6)):753–60.

[18] Lutzelschwab C, Pejler G, Aveskogh M, Hellman L. Secretory granule proteases in rat mast cells. Cloning of 10 different serine proteases and a carboxypeptidase A from various rat mast cell populations. J Exp Med 1997;185(January (1)):13–29.

[19] Hunt JE, Friend DS, Gurish MF, Feyfant E, Sali A, Huang C, et al. Mouse mast cell protease 9, a novel member of the chromosome 14 family of serine proteases that is selectively expressed in uterine mast cells. J Biol Chem 1997;272(November (46)):29158–66.

[20] Aiello RJ, Bourassa PA, Lindsey S, Weng W, Natoli E, Rollins BJ, et al. Monocyte chemoattractant protein-1 accelerates atherosclerosis in apolipoprotein E-deficient mice. Arterioscler Thromb Vasc Biol 1999;19(June (6)):1518–25.

[21] Matsumori A, Furukawa Y, Hashimoto T, Yoshida A, Ono K, Shioi T, et al. Plasma levels of the monocyte chemotactic and activating factor/monocyte chemoattractant protein-1 are elevated in patients with acute myocardial infarction. J Mol Cell Cardiol 1997;29(January (1)):419–23.

[22] Kowalski J, Okopien B, Madej A, Makowiecka K, Zielinski M, Kalina Z, et al. Levels of sICAM-1, sVCAM-1 and MCP-1 in patients with hyperlipoproteinemia IIa and -IIb. Int J Clin Pharmacol Ther 2001;39(February (2)):48–52.

[23] Owen CA, Hu Z, Lopez-Otin C, Shapiro SD. Membrane-bound matrix metalloproteinase-8 on activated polymorphonuclear cells is a potent, tissue inhibitor of metalloproteinase-resistant collagenase and serpinase. J Immunol 2004;172(June (12)):7791–803.

[24] Gueders MM, Balbin M, Rocks N, Foidart JM, Gosset P, Louis R, et al. Matrix metalloproteinase-8 deficiency promotes granulocytic allergen-induced airway inflammation. J Immunol 2005;175(August (4)):2589–97.

Jpn. J. Infect. Dis., 61, 427-433, 2008

Invited Review

Current Risks in Blood Transfusion in Japan

Hiroko Otsubo and Kazunari Yamaguchi*

Department of Safety Research on Blood and Biological Products, National Institute of Infectious Diseases, Tokyo 208-0011, Japan

(Received August 26, 2008)

CONTENTS:

SUMMARY: Over the past decades, the incidence of transfusion-transmitted diseases has been dramatically reduced. These reductions have been due to a multifocal approach to the collection, processing, and release of blood components. The estimated risks of transfusion-transmitted hepatitis viruses are now extremely small, but the possibility of infections with emerging pathogens always exists because preventive measures may not be available for all cases. Thus, some patients may be harmed before preventive measures are introduced. Beside transfusion-transmitted infections (TTI), unsolved residual risks such as transfusion-related acute lung injury or incompatible blood components transfusion still exist as major concerns. Continuous efforts toward research on and the prevention of adverse reaction-related blood components must be made to ensure blood safety. The purpose of this article is to introduce the concept of the current risks of transfusion including TTI, review the preventive measures already implemented, and discuss future visions for transfusion safety in Japan.

1. Introduction

Transfusion safety is of the utmost concern, and much effort has been expended on measures to reduce the risk of transfusion-transmitted infectious agents. Since the onset of the human immunodeficiency virus (HIV) epidemic, effective screening tests have been implemented. Moreover, a multifocal approach to the collection, processing, and release of blood components has been added, and as a result remarkable improvements have been made in blood safety. However, the current strategy could not eliminate all transfusion-transmitted infectious agents, i.e., not only known pathogens but also unknown new agents, and some patients may be harmed before preventive measures are introduced. In Japan, the Japanese Red Cross (JRC), the sole provider of labile blood components in Japan, is responsible for blood products in accordance with the Pharmaceutical Affairs Law and has made much effort to improve blood safety.

*Corresponding author: Mailing address: Department of Safety Research on Blood and Biological Products, National Institute of Infectious Diseases, Gakuen 4-7-1, Musashimurayama, Tokyo 208-0011, Japan. Tel: +81-42-561-0771, Fax: +81-42-561-9722, E-mail: kyama@nih.go.jp

This article is an Invited Review based on a lecture presented at the 18th Symposium of the National Institute of Infectious Diseases, Tokyo, 21 May 2008.

Blood donors should answer many questions about their medical history and their risk factors. Their blood samples should be screened for indicators of infections such as syphilis, parvovirus B19, hepatitis B virus (HBV), hepatitis C virus (HCV), HIV types 1 and 2, and human T-cell lymphotropic virus (HTLV) types I and II. Blood is further tested for cytomegalovirus (CMV) antibody (Ab) before transfusion into patients who are at high risk for CMV disease. Similarly, hepatitis E virus (HEV) is screened as a trial in the Hokkaido district. Even though multifocal approaches to blood safety have been introduced in Japan, unresolved residual risks still exist. These include not only transfusion-transmitted infections (TTI) but also immunological adverse reactions such as transfusion-related acute lung injury (TRALI) and some allergic reactions. For the time being, transfusion components are derived from human blood; therefore, a "zero risk" blood transfusion is never possible. However, it is clear that the application of safety measures and a credible surveillance system which identifies the current transfusion risks will enable transfusion therapy to be safe. A continuous effort toward the research and prevention of adverse reaction-related blood components should be made.

The purpose of this article is to demonstrate the current transfusion risks, describe various approaches that have been implemented for blood safety, and discuss future visions about transfusion medicine in Japan.

2. History of transfusion medicine in Japan

The first transfusion experience in Japan was reported in 1918. Since then, most of the blood components derived from sold blood have been transfused. In 1964, a law came into effect and new JRC statutes were established. At the same time, the Cabinet made a decision that all blood components should be derived from donations, instead of blood sales, and all blood components have been supplied through donated blood since 1969. In 1972, the screening of hepatitis B surface antigen (HBsAg) was begun. The HTLV-I Ab test was added in 1986. In the same year, JRC also began to screen for HIV Abs as a measure to avoid an HIV epidemic.

In 1989, screening strategies for hepatitis B core antibody (HBcAb) and HCVAb were added. JRC established a hemovigilance system in their society and began to collect information on transfusion-related complications including TTI on a voluntary basis in 1993. As a part of the look-back system, JRC began to store 6-ml frozen repository samples from all blood donations in 1996 (1). Since 1999, nucleic acid amplification tests (NAT) for HBV, HCV, and HIV for labile blood products were introduced, and the pool size of NAT was reduced from 500 to 50 the following year (2,3). Since 2004, the pool size of NAT has been reduced from 50 to 20.

In order to investigate the causal relationship between blood components and incidents after transfusion, a look-back system regarding TTI was started nationwide in 2003, and the following year, 6-month-quarantine storage for fresh frozen plasma (FFP) was achieved. In 2005, pre-storage leukocyte-reduction for apheresis-derived platelets was started, and 2 years later, this approach was adapted for all labile blood components. In order to reduce the risk of bacterial contamination, diversion of initial blood flow was adopted in 2006.

Since 2005, people with a history of travel to some European countries, especially England, where bovine spongiform encephalopathy (BSE) is epidemic have been rejected as blood donors.

As noted above, more and more new technologies and/or additional interventions have been adopted over time to achieve the goal of "zero risk."

3. Current risks in transfusion

3-1. Transfusion-transmitted infectious diseases

3-1-1. HBV

Repository samples from all donors, which have been stored since 1996, made it easy to analyze the causal relationship between blood components and recipients. At present, approximately more than 10 cases per year are reported (4) in spite of various approaches to prevent transmission. The NAT-window period (5,6) and low titer of HBV DNA, which cannot be detected in occult HBV-carrier donors, are considered to be the main reasons for this (7-12). A JRC look-back survey reported that the risk of HBV infection caused by blood components from occult HBV carriers with low anti-HBc titers is more than 10-fold lower than the risk caused by donors in the NAT-window periods (6).

According to the JRC reports, it is estimated that the risks of HBV transmission range from 1 in 340,000 bags to 1 in 450,000 bags in Japan (13,14). Satake et al. estimated that the total number of HBV-TTI cases is 17 to 20 per year (1/0.27-0.32 million donations) in Japan out of 5.4 million annual blood donations. This implies that approximately 85% of the HBV infections are caused by donors in the NAT-window period (6).

3-1-2. HCV

Before the implementation of NAT screening, many suspected cases were reported every year. However, during the past few years, one case has been reported every year. The current rate of post-transfusion HCV infection from the donor is estimated to be 1 in 22 million donors, which corresponds to the risk of screening a test-negative, -individual-NAT-positive blood transfusion (13,14).

3-1-3. HIV

One case of HIV transmission due to whole blood transfusion was reported in 1997. Two cases of infected FFP and erythrocytes from the same donor also were reported in 1999. After the implementation of NAT, only one case of FFP-related HIV was reported in 2003. Therefore the risk of transmission is very low, estimated to be 1 in 11 million donors (13,14). However, the number of HIV-infected people in the population has been increasing in Japan. Also, the number of blood donors in which HIV is detected positively has been increasing gradually and finally exceeded 100 people per year in 2007 (Fig. 1) (15).

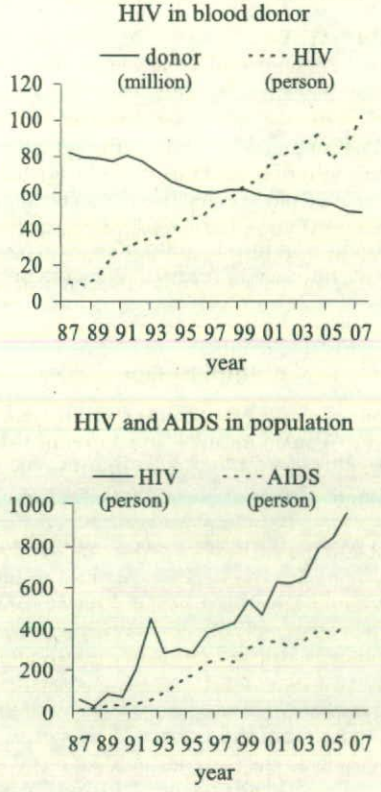

Fig. 1. Trends of the HIV infected rate in population and donation in Japan.

3-1-4. HTLV-I

HTLV-I, the first human retrovirus discovered, is well known as an etiologic pathogen of adult T-cell leukemia/lymphoma (ATL) and other associated diseases. It has been shown to have high seroprevalence in some endemic areas, especially Southwest Japan, the Caribbean islands, and parts of Africa. Its major routes of transmission are considered to be blood transfusion, breast milk feeding and sexual contact (16,17).

Table 1. Previously reported cases of confirmed bacterial contaminated blood components in Japan

Year	Detected bacteria species		Caused blood component
	Patient	Blood component	
1993	*Bacillus subtilis*	NT	RC-MAP
1994	*Serratia marcescens*	NT	PC
1995	*Acinetobacter calcoaceticus*	NT	RC-MAP
1996	*Staphylococcus aureus*	NT	PC
1996	G(+) rod	NT	RC-MAP
1998	*Morganella morganii*	NT	PC
2000	*Bacillus cereus*	*Bacillus cereus*	RC-MAP
2000	*Streptococcus pneumoniae*	*Streptococcus pneumoniae*	PC
2003	*Yersinia enterocolitica*	*Yersinia enterocolitica*	RC-MAP
2006	*Yersinia enterocolitica*	*Yersinia enterocolitica*	RC-MAP
2006	*Yersinia enterocolitica*	*Yersinia enterocolitica*	RC-MAP
2006	*Staphylococcus aureus*	*Staphylococcus aureus*	PC

RC-MAP, erythrocyte concentrate in mannitol-adenine-phosphate solution; PC, platelet concentrates; NT, not tested.

Therefore, preventive measures involving particle agglutination (PA) were implemented in 1986. Moreover, a second generation of PA methods was released for donor screening. Inaba et al. evaluated the efficacy of this screening and HTLV-I prevalence in blood donors after screening estimated the prevalence to be 1 in 45,560 (0.0022%) (18). No confirmed case transmitted by blood components has been reported to the JRC; however, its long latent period and transmission routes other than transfusion make the prevention rate uncertain.

3-1-5. Bacteria

Transfusion-transmitted bacterial contamination of platelets is the most common cause of fatality-related blood components, because the storage of platelets at room temperature to maintain its function is also suitable for bacterial growth. Therefore, numerous countries have introduced culturing-based screening methods to detect bacterial-contaminated platelets. However, after the implementation of these methods, death from bacterial sepsis has continued to be reported because erythrocytes are not screened for bacteria, and current screening methods based on culturing are not entirely satisfactory.

In the United States (US), before the implementation of culturing methods, an average of 11.7 deaths from sepsis per year were reported, whereas 7.5 per year were reported after these detection methods were introduced (19). According to the 6 years' experience of using the BacT/ALERT system in the US, between 0.03 and 0.12% of platelet concentrates (PCs) with a negative culturing test result were still contaminated with bacteria, i.e., false negatives were reported (20).

In Japan, screening methods for platelets have not yet been introduced. We evaluated the efficacy of DOX™ (Daikin Industries, Osaka, Japan), a commercially available system which has been developed to detect contaminated food by measuring the oxygen potential for contaminated PCs. Six species were inoculated into PC, and their dissolved oxygen potentials were measured consecutively (21,22). As a result, this system detected aerobic bacteria in PC within 20 h if their initial concentration was more than 10^1 CFU/ml.

Fatalities from bacterial sepsis are extremely rare and have been reported once every few years (23). However, we have experienced two fatalities from bacterial-contaminated platelet recently. One case was reported in 2000, caused by *Streptococcus pneumoniae* (24), and another case occurred in 2003, caused by a *Staphylococcus aureus*-contaminated platelet (25). In both cases, the patients suffered from malignant hematological diseases. Reported cases of bacterial contamination in Japan are described in Table 1. Since 2007, pre-storage leukocyte-reduction procedure and diversion of initial blood flow have been introduced in Japan. According to the JRC's report, nearly 6,000 blood aliquots from whole blood collected by either the conventional method or from the initial drawn blood flow were cultured using an automated culture system. As a result, the detected rate of bacterial contamination was remarkably reduced from 7 of 2,967 samples (0.24%) to 2 of 2,890 samples (0.07%) after implementation of the diversion (26).

National Blood Service (NBS) in the United Kingdom (UK) also reported that diversion together with improved donor arm disinfection has improved the reduction rate in contamination from 47 to 77% (27).

3-1-6. Prion and other emerging pathogens

Variant Creutzfeldt-Jacob disease (vCJD) was first identified in 1996 in the UK (28,29), and it is considered to be the result of human exposure to the BSE agent. Since then, vCJD patients have been identified in many European countries, especially in the UK. In 2004, the reports showed that vCJD can be transmitted by blood transfusions (30,31). The strategy for preventing trasmission through transfusion has been difficult because there is no effective screening method to determine if a blood donor is infected, and this disease has a long incubation period. Therefore, patients probably received blood products from donors who were asymptomatic at the time of donation. The US instituted a policy in which donations from people who spent at least 6 months in certain western European countries or 3 months in the UK between 1980 and 1996 were excluded. A similar policy has been applied to potential donors in many countries. In Japan, people who spent even one day in the UK from 1980 to 1996 and cumulative periods of 6 months in western European countries where BSE is epidemic were rejected as blood donors.

Consequently, donor deferral was roughly o 6% as a result of this policy. Recently, a number of companies have been developing prion removal filters. Asahi Kasei Medical Co., Ltd. (Tokyo, Japan) has developed an integrated filter which has the functions of prion removal and leukocyte reduction (32,33).

Pall Co., Ltd. (East Hills, N.Y., USA) gained a Council of

Europe (CE) mark for their device "Pall Leukotrap Affinity Prion Reduction Filter (LAPRF)," a new leukocyte reduction filter for the removal of infectious prion from erythrocyte concentrates in 2005 (34,35). Pathogen Removal and Diagnostic Technologies, Inc. (PRDT), which is a joint venture company of the American Red Cross and ProMetic BioSciences, established "P-Capt," which has high prion-binding affinity and also received CE mark in 2006, in cooperation with Macopharma (36).

Some pathogen agents carried by mosquitoes, such as chikungunya virus in the Indian Ocean, West Nile virus in the US, and malaria are widely known as transmitted infectious pathogens (37). Fortunately, this is not an issue of concerne in Japan at present, but potential donors move frequently throughout the world, and some materials imported from abroad may carry mosquitoes. We are collecting information carefully, and we have to manage them in the near future.

Similarly, HEV has been considered to be an imported infectious disease from its epidemic area in the developed countries. However, the epidemiologic study revealed that 2-14% of healthy populations were anti-HEV IgG positive (38), and approximately 13% of the non-A, -B, and -C acute hepatitis cases in Japan were caused by HEV (39). Moreover, the discovery in 2001 of an indigenous Japanese strain of HEV, JRA1, from a patient who had never been abroad, had a great impact on blood safety in our country (40,41). Under these circumstances, HEV screening using a real-time reverse transcription (RT)-polymerase chain reaction (PCR) system has continued as a trial in the Hokkaido district, northern part of Japan.

Blood is also tested for CMV Ab and provided to patients who are at an increased risk for CMV disease in Japan.

3-2. Non-infectious reactions

3-2-1. Hemolytic reactions

Hemolytic reactions are classified into acute hemolytic reactions and delayed hemolytic reactions. Most important hemolytic reactions involve incorrect blood components (IBCT). IBCT has rarely been reported to JRC as an adverse reaction, because it is regarded as a transfusion error. The surveillance of ABO-incompatible blood transfusions was conducted based on an anonymous questionnaire by the Japanese Society of Blood Transfusion for 5 years from 2000 to the end of 2004 (42). This surveillance targeted 1,355 hospitals in Japan, and data were obtained from 829 hospitals among them (61.2%). According to the data, 60 cases of ABO-incompatible transfusion were reported, and 31 of them involved erythrocyte concentrates. Of 31 cases, 22 were due to major mismatches, and others were due to minor mismatches. The current incidents collection system used by JRC is based on voluntary reporting; therefore, the number of reported IBCT cases might be underestimated.

3-2-2. Non-hemolytic reaction

Minor allergic reactions such as urticaria, fever, and dyspnea make up a major portion of non-hemolytic reactions. These include transfusion-associated graft versus host diseases (TA-GVHD) and TRALI.

3-2-3. TA-GVHD

Once TA-GVHD occurs, it is almost always fatal with a very rapid and fulminant course. The mechanism of this condition involves the activation of donor lymphocytes against recipient human leukocyte antigens (HLA). The risk increases in proportion to the degree of HLA haplotype-sharing between donors and patients. In Japan, this condition is a serious problem. Indeed, its incidence is 5-10 times higher than in European countries (43,44). JRC collected information and conducted a national survey in 1991, and a microsatellite DNA assay to identify TA-GVHD has also been developed (45-47). Consequently, JRC has begun the practice of irradiating the blood components supply throughout the country. Since 2000, no confirmed TA-GVHD case has been reported to JRC.

3-2-4. TRALI

TRALI is a serious clinical syndrome involving shortness of breath, hypoxemia and non-cardiogenetic pulmonary edema, associated with HLA/Abs or neutrophil antigens. JRC has gathered information on TRALI since 1997. As knowledge of TRALI has grown, the number of reported TRALI cases has increased. However, the definition of TRALI remains controversial, and it is likely that only a portion of TRALI cases are collected. Other similar serious symptoms which are not included in the definition occur, and treatments have not been developed. Supportive diagnostic evidence includes identifying neutrophil or HLA Abs in the donor or recipient plasma. Among the blood donors, multiparous women frequently have these antibodies. Therefore, in many developed counties, women are not permitted to be plasma donors. In Japan, however, this policy has not been applied.

4. Traceability of causal relationship between blood components and incidents by JRC

JRC has conducted the following tests on residual blood products, plasma derivatives, and recipient blood to identify the causes of adverse reactions and infectious diseases. The contents of the current tests to trace such causes are described in Table 2 (48).

Table 2. Currently conducted tests to identify the causal relationship between blood products and adverse reaction after transfusion according to the classification of reaction type

1. Transmitted infectious diseases
A. Virus
1. Serological test: serological markers related to suspected infections
2. NAT: (1) Detection of suspected viral genome
(2) Evaluation of viral genome sequence homology
B. Bacteria
1. Detection of bacteria by methods based on blood culturing
2. Identification of bacterial species by Gram's stain
3. Detection of endotoxins of Gram-negative bacteria
2. Non-infectious diseases
A. Non-hemolytic adverse reaction
1) Allergic reaction
1. Anti-human leukocyte antigen antibody
2. Anti-platelet antibody
3. Anti-granulocyte antibody
4. Anti-plasma protein antibody: against 6 plasma proteins, including anti-haptoglobin (HP) antibody and anti-immunoglobulin A (IgA) antibody
5. Plasma protein deficiency
2) TA-GVHD
1. Micro-satellite DNA assay
2. Chimerism test on recipient blood
B. Hemolytic adverse reaction
1. Re-check of the blood group and Coombs test
2. Detection of irregular antibody

NAT, nucleic acid amplification tests; TA-GVHD, transfusion-associated graft versus host diseases.

5. Detection strategy versus pathogen reduction for transmitted diseases

At present, detection strategies such as screening tests for known pathogens for which the methods have already been developed are added yearly to maintain the blood components' safety. However, the current strategy does not prevent all of the transfusion-transmitted pathogens. Considering that the use of human blood as a raw biological source is unsafe, screening tests alone cannot exclude all of the potential pathogens. Therefore, we have to consider the introduction of some alternative or additional preventive measures. Some pathogen reduction systems to damage pathogen nucleic acids to proliferate have been developed and some are now under development. Pathogen inactivation (PI) technology using methylene blue plus visible light or solvent-detergent treatment for plasma has been introduced in some European countries and has a track record of more than 10 years (49-51). Similar technologies involving amotosalen (S-59) plus ultraviolet (UV) A light have recently become available for plasma (52). Only amotosalen and riboflavin UV light treatment have obtained the CE mark in Europe, and they have been under evaluation for use with platelets (53,54). With regard to these methods, concern remains regarding cost, process operation changes, ability to inactivate, and ineffectiveness against prions, non-enveloped viruses, spore-formed bacteria and viruses which exist in exceedingly high concentrations in blood. Damage to the products which results in reduction of coagulation factor activities, deterioration of platelets, toxicity, and mutagenicity in recipients is also controversial (55-57). These residual risks are still a major concern to the public, politicians, regulatory agencies, and blood component providers. A recent consensus conference recommended that PI should be implemented when a feasible and safe method to inactivate a broad spectrum of infectious agents is available (58-60).

In Japan, the delegates on behalf of the Japanese Society of Transfusion Medicine and Cell Therapy (JSTMCT) visited some European countries and collected the current information. Additional detection strategies and undeveloped pathogen reduction technology will be extensively debated over the next few years. But it is obvious that TTI is not static and new agents continue to emerge; therefore, we have to carefully watch the circumstances and collect worldwide information.

6. Hemovigilance

Since the AIDS epidemic, developed countries, especially in Europe, took swift action to try to keep records related to transfusion therapy to help ensure blood safety. One method for doing so is called hemovigilance, which is a system for collecting information on unexpected events from donors after drawing blood to the adverse reactions of the patients after transfusion. Various hemovigilance models are usede around the world, depending on social security and national priorities (61-64). JRC has collected transfusion reaction and infectious disease transmission data since 1993, in accordance with the Pharmaceutical Affairs Law. Reporting by medical institutions is voluntary and targets relatively moderate to severe adverse events.

In 2007, JSTMCT established a hemovigilance committee to cooperate with medical institutions and JRC. Seven university hospitals agreed to report all adverse transfusion events

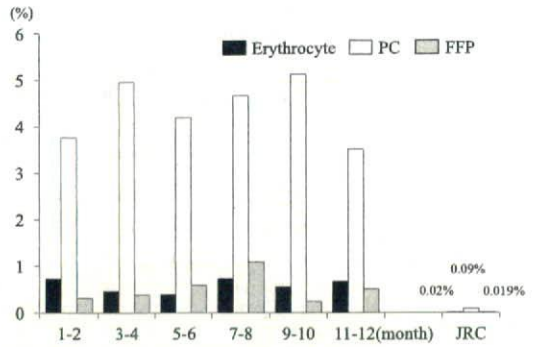

Fig. 2. Bimonthly variability in the reporting rate according to the responsible blood components. PC, platelet concentrates; FFP, fresh frozen plasma.

bimonthly through an anonymous, secure, online portal. Participants also entered the total number of blood products issued over each reporting period. Online access and data entry were made easy, with 16 categories of symptoms and 8 diagnoses. Adverse event rates were calculated automatically and were provided to the participants continuously. As a result of this pilot study, the total number of blood products issued corresponded to about 1% of the total issued in Japan. Six hundred seventy-five transfusion-related adverse events were reported in 2007 by 7 hospitals. Most of them were non-hemolytic transfusion reactions. The reported reaction rates were 0.54 and 0.63% for erythrocytes and plasma, respectively, and 3.4% for PCs in this trial. On the other hand, 0.02% for erythrocytes, 0.018% for plasma, and 0.09% for PCs were nationally reported to JRC (Fig. 2). Hemovigilance such as in this system by a third-party service through an anonymous online portal revealed a high incidence of adverse events, including relatively mild reactions, which physicians previously thought unnecessary, meaningless, or bothersome to report to JRC. Easy online access, anonymity, and the motivation of participating institutions likely contributed to this outcome. This system and the preexisting JRC hemovigilance will complement each other, or rather achieve a better harmonization for future hemovigilance systems (65,66).

7. Conclusion

Current multifocal approaches to blood safety have dramatically reduced the risks related to blood transfusion. However, residual low risks are still a major concern, and we are under pressure to maintain blood product safety. Current approaches have had limited success, and the source of the blood products is raw human blood. In order to improve the safety of blood products, we need to adopt safer alternatives and/or additional preventive measures. Each country has its own circumstances, such as politics, manufacturing, medical resources, and social services, related to transfusion medicine, and each country must develop its most suitable solution.

Consequently, one action taken in one country would not necessarily be an appropriate procedure in another country. It is important to share information and develop standards in transfusion medicine worldwide. However, it is important to remain focused on blood product safety and to track the effectiveness of our policies at all times.

REFERENCES

1. Satake, M. (2007): Japanese repositories. Transfusion, 47, 1105.
2. Mine, H., Emura, H., Miyamoto, M., et al. (2003): High throughput screening of 16 million serologically negative blood donors for hepatitis B virus, hepatitis C virus and human immunodeficiency virus type-I by nucleic acid amplification testing with specific and sensitive multiplex reagent in Japan. J. Virol. Methods, 112, 145-151.
3. Tomono, T., Murokawa, H., Minegishi, K., et al. (2002): Status of NAT screening for HCV, HIV and HBV: experience in Japan. Dev. Biol., 108, 29-39.
4. Japanese Red Cross (2008): JRC News, 0807-113.
5. Satake, M. (2004): Infectious risks associated with the transfusion of blood components and pathogen inactivation. Int. J. Hematol., 80, 306-310.
6. Satake, M., Taira, R., Yugi, H., et al. (2007): Infectivity of blood components with low hepatitis B virus DNA levels identified in a lookback program. Transfusion, 47, 1197-1205.
7. Goyama, S., Kanda, Y., Nannya, Y., et al. (2002): Reverse seroconversion of hepatitis B virus after hematopoietic stem cell transplantation. Leuk. Lymphoma, 43, 2159-2163.
8. Degos, F., Lugassy, C., Degott, C., et al. (1998): Hepatitis B virus and hepatitis B-related viral infection in renal transplant recipients. Gastroenterology, 94, 151-156.
9. Webster, A., Brenner, M.K., Prentice, H.G., et al. (1989): Fatal hepatitis B reactivation after autologous bone marrow transplantation. Bone Marrow Transplant., 4, 207-208.
10. Tsutsumi, Y., Kawamura, T., Saitoh, S., et al. (2004): Hepatitis B virus reactivation in a case of non-Hodgkin's lymphoma treated with chemotherapy and rituximab: necessity of prophylaxis for hepatitis B virus reactivation in rituximab therapy. Leuk. Lymphoma, 45, 627-629.
11. Hourfar, M.K., Walch, L.A., Geusendam, G., et al. (2008): Sensitivity and specificity of anti-HBc screening assays-which assay is best for blood donor screening? Int. J. Lab. Hematol., 30.
12. Kino, K., Tomoda, Y., Ito, R., et al. (2007): Reactivation of hepatitis B virus (HBV) in a multi-transfused patient –confirmation by look-back study using stored specimens–. Jpn. J. Transfus. Cell Ther., 53, 553-557 (text in Japanese).
13. Japanese Red Cross (2005): JRC News, 0506-89.
14. Tadokoro, K. (2007): The new Japanese blood law: its impact on blood safety and usage. Dev. Biol., 127, 161-168.
15. Ministory of Health, Labour and Welfare. Online at <http://api-net.jfap.or.jp/mhw/survey/07nenpo/kensu.pdf> (in Japanese).
16. Lefrere, J.J. (2000): Human T-lymphotropic virus type I (HTLV-I): risk of transmission with transfusion. Presse Med., 10, 1134-1138.
17. Yamaguchi, K. (1994): Human T lymphotropic virus type-I in Japan. Lancet, 343, 213-216.
18. Inaba, S., Okochi, K., Sato, H., et al. (1999): Efficacy of donor screening for HTLV-I and the natural history of transfusion-transmitted infection. Transfusion, 39, 1104-1110.
19. Blajchman, M.A. and Vamvakas, E.C. (2006): The continuing risk of transfusion-transmitted infections. N. Engl. J. Med., 355, 1303-1305.
20. Larsen, C.P., Ezligini, F., Hermansen, N.O., et al. (2005): Six years' experience of using the BacT/ALERT system to screen all platelet concentrates, and additional testing of outdated platelet concentrates to estimate the frequency of false-negative results. Vox Sang., 88, 93-97.
21. Otsubo, H., Yamaguchi, K. and Hoshi, Y. (2008): Consecutive monitoring of dissolved oxygen consumption by DOX™ system to evaluate bacterial contamination in platelet concentrates. Jpn. J. Transfus. Cell Ther., 54, 372-377 (text in Japanese).
22. Otsubo, H., Sasaki, Y., Yamaguchi, K., et al. (2007): Consecutive monitoring of dissoleved oxygen consumption by DOX™ to evaluate bacteria in platelet concentrates. Transfusion, 47 (3S), 205A.
23. Takahashi, M. and Nagumo, H. (2008): Septic transfusion reaction resulting from bacterial contamination of blood components. Jpn. J. Transfus. Cell Ther., 54, 359-371 (text in Japanese).
24. Katayama, T., Kamiya, M., Hoshina, S., et al (2003): Fatal septic shock and rhabdomyolysis following transfusion of platelet concentrates contaminated with *Streptococcus pneumoniae*. Rinsho Ketsueki, 44, 381-385 (in Japanese).
25. Uruma, M., Kato, H., Ando, T., et al. (2008): A fatal case of sepsis caused by MSSA contamination of platelet concentrate. Jpn. J. Transfus. Cell Ther., 54, 38-42 (text in Japanese).
26. Nagumo, H., Shinozaki, K., Kimura, Y., et al. (2007): The effect of diversion of first blood volume on the frequency of bacterial contamination in whole blood collection. Jpn. J. Transfus. Cell Ther., 53, 598-601 (text in Japanese).
27. McDonald, C.P. (2006): Bacterial risk reduction by improved donor arm disinfection, diversion and bacterial screening. Transfus. Med., 16, 381-396.
28. Will, R.G., Ironside, J.W., Zeidler, M., et al. (1996): A new variant of Creutzfeldt-Jacob disease in the UK. Lancet, 6, 921-925.
29. Zeidler, M., Stewart, G.E., Barraclough, C.R., et al. (1997): New variant Creutzfeldt-Jacob disease: neurological features and diagnostic tests. Lancet, 27, 350, 903-907.
30. Paden, A.H., Head, M.W., Ritchie, D.L., et al. (2004): Preclinical vCJD after transfusion in a PRNP codon 129 heterozygous patient. Lancet, 364, 527-529.
31. Hewitt, P.E., Llewelyn, C.A., Mackenzie, J., et al. (2006): Creutzfeldt-Jacob disease and blood transfusion: result of the UK transfusion medicine epidemiological review study. Vox Sang., 91, 221-230.
32. Prowse, C. (2006): Prion removal with filters. Vox Sang. ISBT Science Series 2006 (1), 230-234.
33. Yokomizo, T., Nirasawa, H., Kai, T., et al. (2008): A combination filter for prion and leukocyte reduction, its applicability as an integral filter with blood bag systems. Vox Sang., 95 (Suppl. 1), 271.
34. Sowemimo-Coker, S.O., Pesci, S., Andeade, F., et al. (2006): Pall leukotrap affinity prion-reduction filter removes exogenous infectious prions and endogenous infectivity from red cell concentrares. Vox Sang., 90, 265-275.
35. Sowemimo-Coker, S., Kascsak, R., Kim, A., et al. (2005): Removal of exogenous (spiked) and endogenous prion infectivity from red cells with a new prototype of leukoreduction filter. Transfusion, 45, 1839-1844.
36. Gregori, L., Lambert, B.C., Gugel, P.V., et al. (2006): Reduction of transmissible spongiform encephalopathy infectivity from human red blood cells with prion protein affinity ligands. Transfusion, 46, 1152-1161.
37. Rezza, G., Nicoletti, L., Angelini, R., et al.(2007): Infection with chikungunya virus in Italy: an outbreak in a temperate region. Lancet, 370, 1840-1846.
38. Li, T.C., Zhang, J., Shinzawa, H., et al. (2000): Empty virus-like particle-based enzyme-linked immunosorbent assay for antibodies to hepatitis E virus. J. Med. Virol., 62, 327-333.
39. Mizuo, H., Suzuki, K., Takikawa, Y., et al. (2002): Polyphyletic strains of hepatitis E virus are responsible for sporadic cases of acute hepatitis in Japan. J. Clin. Microbiol., 40, 3209-3218.
40. Matsubayashi, K., Nagaoka, Y., Sakata, H., et al. (2004): Transfusion-transmitted hepatitis E caused by apparently indigenous hepatitis E virus strain in Hokkaido, Japan. Transfusion, 44, 934-940.
41. Matsubayashi, K., Kang, J.H., Sakata, H., et al. (2008): A case of transfusion-transmitted hepatitis E caused by blood from a donor infected with hepatitis E virus via zoonotic food-borne route. Transfusion, 48, 1368-1375.
42. Fujii, Y., Matsuzaki, M., Miyata, S., et al. (2007): Analysis of the causes of ABO-incompatible transfusion in Japan. Jpn. J. Transfus. Cell Ther., 53, 374-382 (text in Japanese).
43. Aoun, E., Shamseddine, A., Chehal, A., et al. (2003): Transfusion-associated GVHD: 10 years' experience at the American University of Beirut-Medical Center. Transfusion, 43, 1672-1676.
44. Williamson, L.M., Stainsby, D., Jones, H., et al. (2007): The impact of universal leukodepletion of the blood supply on hemovigilance reports of posttransfusion purpura and transfusion-associated graft-versus-host diseases. Transfusion, 47, 1455-1467.
45. Ryo, R., Saigo, K., Hashimoto, M., et al. (1999): Treatment of post-transfusion graft-versus-host diseases with Nafmostat Mesilate, a serine protease inhibitor. Vox Sang., 76, 241-246.
46. Nishimura, M., Hidaka, N., Akaza, T., et al. (1998): Immunosuppressive effects of chloroquine: potential effectiveness for treatment of post-transfusion graft-versus-host diseases. Transfus. Med., 8, 209-214.
47. Juji, T., Nishimura, M. and Tadokoro, K. (2000): Treatment of post transfusion graft-vesus-host diseases. Vox Sang., 78, (Suppl. 2), 277-279.
48. Okazaki, H. (2007): The benefits of the Japanese haemovigilance system for better patient care. Vox Sang., ISBT Science Series, 104-109.
49. Seghatchian, J., Walker, W.H. and Reichenberg, S. (2008): Updates on pathogen inactivation of plasma using Theraflex methylene blue system. Transfus. Apher. Sci., 38, 271-280.
50. Solheim, B.G. and Seghatchian, J. (2006): Update on pathogen reduction technology for therapeutic plasma: an overview. Transfus. Apher. Sci., 35, 83-90.
51. Politis, C., Kavallierou, L., Hantziara, S., et al. (2007): Quality and safety of frozen plasma inactivated and leucoreduced with the theraflex methylene blue system including the Blueflex filter: 5 years' experience. Vox Sang., 92, 319-326.
52. Herving, T.A., Apelseth, T. and Sondergaard, M. (2006): Plasma/platelet pathogen inactivation. ISBT Science Series, 1, 227-229.
53. Pineda, A., McCullough, J., Benjamin, R.J., et al. (2006): Pathogen inactivation of platelets with a photochemical treatment with amotosalen

HCL and ultraviolet light: process used in the SPRINT trial. Transfusion, 46, 562-571.
54. McCullough, J. (2006): Pathogen inactivation of platelets. Transfus. Altern. Transfus. Med., 2, 121-126.
55. Solheim, B.G. (2008): Pathogen reduction of blood components. Transfus. Aphere. Sci., 39, 75-82.
56. Rio-Garma, J., Alvarez-Larran, A., Martinez, C., et al. (2008): Methylene blue-photoinactivated plasma versus quarantine fresh frozen plasma in thrombotic thrombocytopenic purpura: a multicentric, prospective cohort study. Br. J. Haematol., 1-7.
57. Seghatchian, J. and Sousa, G. (2006): Pathogen-reduction systems for blood components: the current position and future trends. Transfus. Apher. Sci., 35, 189-196.
58. Webert, K.E., Cserti, C.M., Hannon, J., et al. (2008): Proceeding of a consensus conference: pathogen inactivation making decisions about new technologies. Transfus. Med. Rev., 22, 1-34.
59. Klein, H.G., Anderson, D., Bernardi, M.J., et al. (2007): Pathogen inactivation: making decisions about new technologies-report of a consensus conference. Transfusion, 47, 2338-2347.
60. Klein, H.G., Bernardi, M.J., Cable, R., et al. (2007): Pathogen inactivation: making decision about new technologies-preliminary report of a consensus conference. Vox Sang., 93, 179-182.
61. Andreu, G., Morel, P., Forestier, F., et al. (2002): Hemovigilance network in France: organization and analysis of immediate transfusion incident reports from 1994 to 1998. Transfusion, 42, 1356-1364.
62. Migeot, V., Tellier, S. and Ingrand, P. (2003): Diversity of bedside pretransfusion ABO compatibility devices in metropolitan France. Transfus. Clin. Biol., 10, 26-36.
63. Stansby, D., Jones, H., Asher, D., et al. (2006): Serious hazard of transfusion: a decade of hemovigilance in the UK. Transfus. Med. Rev., 20, 273-282.
64. Faber, J.C. (2004): Work of the European Haemovigilance Network (EHN). Transfus. Clin. Biol., 11, 2-10.
65. Otsubo, H., Hamaguchi, I. and Yamaguchi, K. (2008): Hemovigilance and blood safety control. J. Med. Tech., 52, 157-161.
66. Otsubo, H., Kato, H., Yonemura, Y., et al.: Better building hemovigilance system in Japan. Jpn. J. Transfus. Cell Ther. (text in Japanese) (in press).

The American Journal of Pathology, Vol. 172, No. 6, June 2008

DOI: 10.2353/ajpath.2008.071060

Immunopathology and Infectious Disease

Mouse-Passaged Severe Acute Respiratory Syndrome-Associated Coronavirus Leads to Lethal Pulmonary Edema and Diffuse Alveolar Damage in Adult but Not Young Mice

Noriyo Nagata,* Naoko Iwata,* Hideki Hasegawa,* Shuetsu Fukushi,† Ayako Harashima,* Yuko Sato,* Masayuki Saijo,† Fumihiro Taguchi,‡ Shigeru Morikawa,† and Tetsutaro Sata*

From the Departments of Pathology, Virology I,† and Virology III,‡ National Institute of Infectious Diseases, Musashimurayama, Tokyo, Japan*

Advanced age is a risk factor of severe acute respiratory syndrome (SARS) in humans. To understand its pathogenesis, we developed an animal model using BALB/c mice and the mouse-passaged Frankfurt 1 isolate of SARS coronavirus (SARS-CoV). We examined the immune responses to SARS-CoV in both young and adult mice. SARS-CoV induced severe respiratory illness in all adult, but not young, mice on day 2 after inoculation with a mortality rate of 30 to 50%. Moribund adult mice showed severe pulmonary edema and diffuse alveolar damage accompanied by virus replication. Adult murine lungs, which had significantly higher interleukin (IL)-4 and lower IL-10 and IL-13 levels before infection than young murine lungs, rapidly produced high levels of proinflammatory chemokines and cytokines known to induce macrophage and neutrophil infiltration and activation (eg, tumor necrosis factor-α). On day 2 after inoculation, young murine lungs produced not only proinflammatory cytokines but also IL-2, interferon-γ, IL-10, and IL-13. Adult mice showed early and acute excessive proinflammatory responses (ie, cytokine storm) in the lungs after SARS-CoV infection, which led to severe pulmonary edema and diffuse alveolar damage. Intravenous injection with anti-tumor necrosis factor-α antibody 3 hours after infection had no effect on SARS-CoV infection. However, intraperitoneal interferon-γ injection protected adult mice from the lethal respiratory illness. The experimental model described here may be useful for elucidating the pathophysiology of SARS and for evaluating therapies to treat SARS-CoV infection. *(Am J Pathol 2008, 172:1625–1637; DOI: 10.2353/ajpath.2008.071060)*

In the severe acute respiratory syndrome-associated coronavirus (SARS-CoV) epidemic of winter 2002 to 2003, ~800 people (10% of the >8000 SARS patients) suffered progressive respiratory failure and died.[1–5] Common symptoms of SARS include fever, nonproductive cough, myalgia, and dyspnea. An age of 60 years or older, co-morbid disease, male sex, high neutrophil counts, and several biochemical abnormalities are associated with poor outcomes.[6–10]

The SARS-CoV spike (S) protein mediates the infection of cells bearing an appropriate receptor.[11] One such receptor is angiotensin-converting enzyme 2 (ACE2), which binds SARS-CoV S protein with high affinity.[11–14] That the binding of SARS-CoV to ACE2 may contribute to SARS-CoV-associated pathology is suggested by several reports showing that angiotensin II expression promotes severe lung failure on acute lung injury whereas ACE2 expression protects from lung injury.[15,16] However, it is likely that the acute lung injury caused by SARS-CoV infection is also attributable to a complex pathophysiological process in which inflammatory cytokines released by activated alveoli macrophages induce immune system dysregulation.[17–20]

To understand the pathogenesis of SARS-CoV, the SARS-CoV susceptibility of experimental animals such as monkeys, cats, ferrets, mice, pigs, guinea pigs, ham-

Supported by the Ministry of Health, Labor, and Welfare, Japan (grant-in aid for research on emerging and re-emerging infectious diseases); and the Ministry of Education, Culture, Sports, Science, and Technology, Japan (grant-in-aid for scientific research no. 17790313).

Accepted for publication February 22, 2008.

Supplemental material for this article can be found on *http://ajp.amjpathol.org*.

Address reprint requests to Noriyo Nagata, D.V.M., Ph.D., Department of Pathology, National Institute of Infectious Diseases, Gakuen 4-7-1, Musashimurayama, Tokyo 208-0011, Japan. E-mail: nnagata@nih.go.jp.

sters, chickens, and rats has been investigated.[2,4,21–28] All of these animals are susceptible to SARS-CoV after intrarespiratory inoculation and exhibit virus excretion in pharyngeal or nasal swabs, histopathological pulmonary lesions, and seroconversion. However, the course of infection in these animals is shorter than that in humans.

As in humans, an advanced age correlates positively and independently with adverse outcomes and is a predictor of mortality in animal models.[6–10] Moreover, SARS-CoV isolates replicate better in aged BALB/c mice than in younger mice.[29] It is likely that the correlation between poor outcome and advanced age reflects the weakened immune responses of the elderly, in particular their impaired cytokine responses. This is significant because cytokines regulate the immune response to infection. Indeed, analysis of the cytokine responses of elderly individuals to respiratory infections that lead to severe pulmonary diseases (eg, *Listeria monocytogenes*, respiratory syncytial virus, influenza virus)[30–33] have revealed unbalanced Th1-type and Th2-type responses.

We recently succeeded in establishing a rat model of SARS using rat-passaged SARS-CoV.[34] Although the rat-passaged SARS-CoV was not lethal, it induced more severe pathological lesions in adult F344 rats than in young rats. We found that the severe inflammation in the adult rats was associated with high levels of inflammatory cytokines in the serum and lung homogenates, especially interleukin (IL)-6, along with low levels of the immunosuppressive cytokine IL-10. IL-6 is an inflammatory cytokine that is produced by monocytes, leukocytes, endothelial cells, fibroblasts, and alveolar epithelial cells. SARS patients have significantly elevated serum IL-6 levels.[19] IL-10 is produced by macrophages, Th2 lymphocytes, and B cells and inhibits tumor necrosis factor (TNF)-α production and neutrophil activation in lipopolysaccharide-induced acute lung injury, thereby suppressing lung tissue injury.[35] It has been reported that serum IL-10 levels increase in SARS patients during the convalescence phase.[19]

In this study, we established a new and more useful experimental small animal model for SARS by using BALB/c mice and mouse-passaged SARS-CoV. This model allows us to better characterize the virus-host relationship and determine which immune responses are antiviral and which are pathogenic. Here, we sought to determine why SARS-CoV infection is more frequently lethal in elderly patients by comparing SARS-CoV-infected adult and young mice in terms of their pulmonary pathology and immune responses.

Materials and Methods

Virus and Cells

The Frankfurt 1 isolate of SARS-CoV used in this study was kindly supplied by Dr. John Ziebuhr, Institute of Virology and Immunology, University of Würzburg, Würzburg, Germany. The virus was propagated twice in Vero E6 cells purchased from American Type Cell Collection (Manassas, VA) that were cultured in Eagle's minimal essential medium (MEM) containing 5% fetal bovine serum, 50 IU of penicillin G, and 50 μg of streptomycin per ml. Titers of this stock virus were expressed as 50% of the tissue culture infectious dose ($TCID_{50}$)/ml on Vero E6 cells, which was calculated according to the Behrens-Kärber method. Work with infectious SARS-CoV was performed under biosafety level 3 conditions. Compared to the original virus, the Frankfurt 1 isolate used in our laboratory has one amino acid change at position 641 (His to Tyr) in the S protein and another in open reading frame (ORF) 1a 429 (Ala to Ser). These changes presumably arose during the passage through Vero E6 cells.

Mice

Female 4-week-old or 6-month-old BALB/c mice were purchased from Japan SLC (Shizuoka, Japan) and maintained in specific pathogen-free facilities. On experimental infection, these animals were housed in biosafety level 3 animal facilities. These animal experiments were approved by the Animal Care and Use Committee of the National Institute of Infectious Diseases, Tokyo, Japan.

Serial in Vivo *Passage of SARS-CoV in Mice*

The Frankfurt 1 isolate of SARS-CoV was serially passaged 10 times in 4-week-old female BALB/c mice, as follows. After intranasal inoculation, three mice were sacrificed on day 3 after inoculation and their bronchoalveolar wash fluids were collected. These bronchoalveolar fluids were then used to inoculate three additional BALB/c mice, whose bronchoalveolar fluids on day 3 after inoculation were used to inoculate fresh mice. After 10 such passages in mice, the lungs were removed under sterile conditions, washed three times, and homogenized in 1 ml of phosphate buffer containing 0.1% bovine serum albumin, 20 IU of penicillin G, 20 μl of streptomycin, and 1 μg of amphotericin B per ml. The lung homogenates were centrifuged at 1000 $\times$ *g* for 20 minutes, and 1 ml of the supernatants in 10 ml of MEM containing 2% fetal bovine serum were used to infect Vero E6 cells. After 1 hour of adsorption, the inoculum was removed and MEM containing 2% fetal bovine serum was added. The cell cultures were incubated at 37°C with 5% CO_2 for 2 days and then treated once with freeze-thawing. After centrifugation at 1000 $\times$ *g* for 20 minutes, the supernatants (referred to here as F-musX-VeroE6) were used as the virus inoculum. Compared to the original virus, F-musX-VeroE6 has amino acid mutations in the S protein at positions 480 (Asp to Glu) and 641 (His to Tyr); The latter change is identical to one of the mutations found in the Frankfurt 1 isolate. In the completely sequenced genome, F-musX-VeroE6 also has two additional mutations in ORF1a 3534 (Phe to Leu) and ORF1ab 5172 (Thr to Ile). The mutation in ORF1a 429 found in the Frankfurt 1 isolate was not present.

Experimental Mouse Infection

Mice were anesthetized by intraperitoneal injection with a 0.1 ml/10 g body weight mixture of 1.0 mg ketamine and

0.02 mg xylazine. The animals were then inoculated intranasally in the left nostril with the Frankfurt 1 isolate or F-musX-VeroE6 (2×10^6 $TCID_{50}$ in 20 μl) and observed for clinical signs. Body weight was measured daily for 10 or 21 days. Infected animals were also sacrificed at various time points after inoculation to analyze virus replication, hematology, cytokine expression, and pathology ($n = 3$ in each group).

Virus Isolation and Titration

Twenty percent (w/v) tissue homogenates of the lung, maxilla (including the nasal cavity), cervical lymph node, spleen, liver, and kidney were prepared in MEM containing 2% fetal bovine serum, 50 IU penicillin G, 50 μg streptomycin, and 2.5 μg amphotericin B per ml (MEM-2FBS). Bronchoalveolar and nasal wash fluids were also collected for analysis of virus replication. Viral infectivity titers of respiratory tract and wash fluids were determined as described above. Virus isolation from other tissues was performed by blind passage after freezing and thawing the first-round passage using Vero E6 cells.

Hematological Analysis

Total blood cell counts in peripheral blood collected in sodium-heparinized tubes were measured by an autoanalyzer (Cell Tuck; Nihon Koden, Tokyo, Japan). Neutrophil, lymphocyte, monocyte, eosinophil, and basophil counts were determined by microscopic analysis.

Flow Cytometric Analysis

Antibodies used for flow cytometry were anti-CD4-phycoerythrin-Cy5 (eBioscience, San Diego, CA), anti-CD8β-phycoerythrin (Santa Cruz Biotechnology, Santa Cruz, CA), and anti-pan-NK cells-fluorescein isothiocyanate (eBioscience). Cells incubated with these surface-binding antibodies were fixed in 2% paraformaldehyde in phosphate-buffered saline (PBS) and subjected to flow cytometry (EPICS Elite; Beckman Coulter, Fullerton, CA) using EXPO cytometer software (Beckman Coulter).

Cytokine Multiplex Analysis

Homogenized lung tissue samples were diluted 1:1 with cell extraction buffer [10 mmol/L Tris, pH 7.4, 100 mmol/L NaCl, 1 mmol/L EDTA, 1 mmol/L EGTA, 1 mmol/L NaF, 20 mmol/L $Na_4P_2O_7$, 2 mmol/L Na_3VO_4, 1% Triton X-100, 10% glycerol, 0.1% sodium dodecyl sulfate, and 0.5% deoxycholate (BioSource International, Inc., Camarillo, CA)], incubated for 30 minutes on ice with vortexing at 10 minute intervals, and then centrifuged at 15,000 $\times$ *g* for 10 minutes at 4°C. Supernatants were diluted 1:5 in assay diluent of the Mouse Cytokine 20-Plex antibody bead kit (BioSource International). Sera and the 20% lung homogenate supernatants were subjected to ultraviolet irradiation for 10 minutes to inactivated virus infectivity and stored at −80°C until they were used to determine the presence of mouse cytokines, namely, basic fibroblast growth factor, GM-CSF, interferon (IFN)-γ, IL-1α, IL-1β, IL-2, IL-4, IL-5, IL-6, IL-10, IL-12p40/p70, IL-13, IL-17, IP-10, keratinocyte chemoattractant (KC), monocyte chemoattractant protein 1 (MCP-1), MIG, MIP-1α, TNF-α, and vascular endothelial growth factor (VEGF), by using the Mouse Cytokine 20-Plex antibody bead kit and Luminex 100TM (Luminex Co., Austin, TX).

Histopathological and Immunohistochemical Analysis

Animals ($n = 3$ in each group) were anesthetized and perfused with 2 ml of 10% phosphate-buffered formalin. Fixed lung, heart, kidney, liver, spleen, small and large intestine, brain, spinal cord, and maxilla (including nasal cavity) tissues were routinely embedded in paraffin, sectioned, and stained with hematoxylin and eosin. Maxilla samples were decalcified in phosphate-buffered saline (pH 7.4) plus 10% EDTA before being embedded. Immunohistochemical detection of the SARS-CoV antigens was performed on paraffin-embedded sections, as follows. After deparaffinizing with xylene, sections were rehydrated in ethanol and immersed in PBS. Antigens were retrieved by hydrolytic autoclaving for 20 minutes at 121°C in 10 mmol/L sodium citrate-sodium chloride buffer (pH 6.0). After cooling, the sections were immersed in PBS. Endogenous peroxidase was blocked by incubation in 1% hydrogen peroxide in methanol for 30 minutes. After washing in PBS, the sections were incubated with normal rabbit serum for 5 minutes, and then with rabbit antibody against SARS-CoV[32,36] overnight at 4°C. After three washes in PBS, the sections were incubated with biotin-conjugated anti-rabbit IgG for 30 minutes at 37°C, followed by reaction with streptavidin-peroxidase for 30 minutes at room temperature. Peroxidase activity was detected by development with diaminobenzidine containing hydrogen peroxide. Nuclei were counterstained by hematoxylin.

Double Immunofluorescence Staining

SARS-CoV- and mock-infected adult and young mice were euthanized 1, 3, and 5 days after inoculation by exsanguination under excess ether anesthesia, after which the lungs were harvested for pathological examination (three mice per group). Mock infection was performed by using MEM containing 2% fetal bovine serum. For staining with anti-Mac-3 and anti-surfactant D (SP-D) antibodies and to detect SARS-CoV antigens, the lungs were fixed with 4% paraformaldehyde in PBS at 4°C for 15 to 18 hours and embedded in paraffin according to the manufacturer's instructions (BD Biosciences Pharmingen, San Diego, CA). The paraffin-embedded sections were then subjected to a double-immunofluorescence staining method[37] using a polyclonal rabbit antibody against SARS-CoV[36] and the SKOT9 monoclonal mouse antibody against nucleocapsid protein[38] or a monoclonal rat anti-Mac-3 antibody against mouse mononuclear phagocytes (BD Biosciences Pharmingen), and a poly-

clonal rabbit anti-SP-D antibody (Chemicon International, Inc., Billerica, MA). Briefly, after deparaffinization with xylene, the sections were rehydrated in ethanol and immersed in PBS. Antigens were retrieved by hydrolytic autoclaving for 10 minutes at 121°C in 10 mmol/L sodium citrate-sodium chloride buffer (pH 6.0). After cooling, the sections were immersed in PBS, and then incubated with primary antibodies overnight at 4°C. To block background staining, normal donkey serum or the M.O.M. immunodetection kit for primary mouse monoclonal antibody (Vector Laboratories, Burlingame, CA) were used according to the manufacturer's instructions. After three washes in PBS, the sections were incubated for 30 minutes at 37°C with biotin-conjugated secondary antibodies, ie, a donkey anti-rat serum (Jackson ImmunoResearch, West Grove, PA) to detect the Mac-3 antibody or a goat anti-rabbit serum (Jackson ImmunoResearch) to detect the SP-D antibody. After three washes in PBS, the sections were incubated with streptavidin-Alexa Fluor 488 (Molecular Probes, Eugene, OR) for 60 minutes at room temperature. After three washes in PBS, to detect the SARS-CoV antibodies (the SKOT9 or the rabbit antibody), the sections were incubated with anti-rabbit or anti-mouse Alexa Fluor 568 (Molecular Probes) for 60 minutes at room temperature. The sections were counterstained with TO-PRO-3 nucleic acid staining (Molecular Probes) and images were captured and analyzed by confocal laser microscopy (Fluoview, FV1000; Olympus, Tokyo, Japan).

Anti-Mouse TNF-α Antibody or IFN-γ Treatment in Vivo

Three hours after intranasal inoculation of F-musX-VeroE6 (2×10^6 $TCID_{50}$ in 20 μl), adult (6-month-old) BALB/c females mice were injected intravenously with 100 μl of anti-mouse TNF-α rat monoclonal antibody (1 μg/μl, Biosource), or isotype-matched control rat antibody (1 μg/μl; MP Biomedicals, Solon, OH) in PBS, or injected intraperitoneally with 100 μl of recombinant mouse IFN-γ (0.05 μg/μl; R&D Systems, Minneapolis, MN) or intraperitoneal injection with 100 μl of PBS/0.1% bovine serum albumin was used as control. At least two independent experiments were performed ($n = 5$ or 8 per group).

Evaluation of Blood Permeability

SARS-CoV- and mock-infected mice were injected intravenously with 100 μl of 1% Evans blue dye (Tokyo Kasei, Tokyo, Japan) 1 hour before sacrifice ($n = 3$ in each group). Mock infection was performed by using MEM containing 2% fetal bovine serum. After perfusion with isotonic saline, the whole lung was removed and immersed in 10% phosphate-buffered formalin. The fixed lungs were immediately frozen in cold acetone with dry ice in 100% O.C.T. compound (Sakura Finetechnical Co. Ltd., Tokyo, Japan). Cryosections (5 μm) (CM1900; Leica, Wetzlar, Germany) were mounted on MAS-coated slides (Matsunami, Osaka, Japan), air-dried, and examined with a fluorescence microscope.

Statistical Analysis

Statistical significance was determined by Student's *t*-test. *P* values <0.05 were considered significant.

Results

The Virulence and Pathogenicity of SARS-CoV in Mice Is Enhanced by Serial Mouse Passaging

The Frankfurt 1 isolate was passaged twice on VeroE6 cells and then serially passaged 10 times in young BALB/c mice (4-week-old females) by intranasal inoculation of bronchoalveolar fluids from infected mice. The F-musX-VeroE6 strain showed higher replication and pathogenicity in the respiratory tract of young BALB/c mice than the original Frankfurt 1 isolate, as follows (Figure 1, A–E). On day 3 after inoculation, F-musX-VeroE6 replication in the lung washes was higher than that of the original Frankfurt 1 isolate ($P = 0.055$) but lower in the nasal washes ($P < 0.01$) (Figure 1A). Compared to Frankfurt 1 isolate-inoculated young mice, the F-musX-VeroE6-inoculated young mice also evinced more lung inflammation, as shown by neutrophil, macrophage, and lymphocyte infiltration and virus antigen-positive cells in the alveolar spaces (Figure 1, B–E). However, the F-musX-VeroE6-inoculated young mice did not develop any obvious respiratory illnesses, although they did show transient weight loss for a few days after inoculation (data not shown).

Because advanced age is associated with higher mortality in human SARS patients and SARS-CoV replicates better in aged mice,[6–10,29] we experimentally infected 6-month-old (adult) female BALB/c mice with F-musX-VeroE6 or the Frankfurt 1 isolate. Although none of the mice showed clinical signs of illness after intranasal inoculation with Frankfurt 1 isolate, all F-musX-VeroE6-inoculated mice became severely ill, as revealed by significant weight loss (~20% of their initial body weight), hunching, ruffled fur, and dyspnea on day 2 after inoculation (Figure 1F). Three of the ten mice became moribund and died of severe respiratory illness on days 3, 6, and 10 after inoculation (30% mortality rate). The surviving animals recovered their body weight during days 4 to 6 after inoculation.

Pathogenesis of Mouse-Passaged SARS-CoV in Young and Adult BALB/c Mice

These results demonstrated that serial *in vivo* passage of SARS-CoV in mice increased the virulence of the virus, especially in adult mice. Thus, we characterized the clinical and pathological features of F-musX-VeroE6-infected young and adult mice up until day 5 after inoculation in more detail. The young mice again showed transient weight loss of up to 8.2% (SD = 3.7%) during days 2 to 4 after inoculation but had recovered their weight by day 5 after inoculation (Figure 2A). In contrast, the adult mice showed continuous weight loss of up to 23.0% (SD =

4.5%) of their initial body weight that continued until day 5 after inoculation. All adult mice showed virtually identical clinical manifestations during days 1 to 2 after inoculation (such as hunching and ruffled fur) that were not observed in the young mice. Severe respiratory symptoms such as dyspnea were also observed in the adult mice from 2 days after inoculation onwards. In this experiment, 50% of the adult mice had died by day 5 after inoculation.

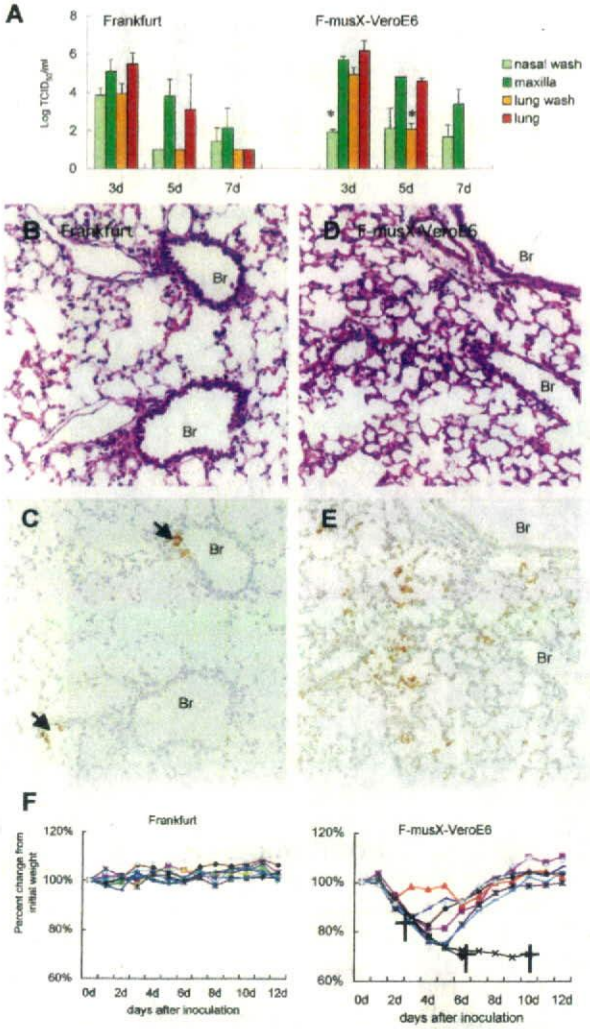

Figure 1. Comparison of the replication and pathogenicity of F-musX-VeroE6 and the original Frankfurt 1 isolate in young (4 weeks old) (**A–E**) and adult (6 months old) (**F**) female BALB/c mice. **A:** Virus titers in nasal wash fluids, homogenates of maxilla (including the nasal cavity), lung wash fluid, and lung homogenates of young mice on days 3, 5, and 7 after inoculation ($n = 3$ per group). The detection limit was $10^{1.5}$ $TCID_{50}$/g of tissue. **Asterisks** indicate statistically significant differences between F-musX-VeroE6 and the Frankfurt isolate ($P < 0.05$). **B–E:** Histopathological features of the lungs of young mice on day 3 after inoculation. **B:** After infection with the Frankfurt 1 isolate, inflammatory infiltrates in the lung were not detected. Moreover, very few alveolar pneumocytes and alveolar duct and alveolus epithelial cells were SARS-CoV antigen-positive (**C**, **arrowheads**). In contrast, extensive cellular infiltration (**D**) and many virus antigen-positive cells (**E**) were seen in the alveolar area after F-musX-VeroE6 infection. **F:** Clinical illness in individual 6-month-old adult BALB/c mice after Frankfurt isolate or F-musX-VeroE6 infection ($n = 10$ per group). Shown are the changes in body weight (expressed as percentages of the body weight on day 0). The mean initial body weight of the two mouse groups (on day 0) were 24.72 ± 1.04 g and 25.44 ± 1.55 g, respectively. Significant differences in body weight change were detected on days 2 to 8 after inoculation. For example, the average body weight F-musX-VeroE6-infected adult mice on day 5 after inoculation was 83.4 ± 9.88% of the mean day 0 body weight. This was significantly lower than the average body weight change of Frankfurt 1 isolate-infected adult mice on day 5 after inoculation (102.4 ± 2.99%). Three F-musX-VeroE6-infected adult mice died (crosses) of severe pulmonary edema on days 3, 6, and 10 after inoculation.

The lungs of infected young and adult mice were weighed on days 0 to 5 after inoculation. The progressive increase in lung weight of the adult mice suggested the development of pulmonary edema (Figure 2, B and C). By day 5 after inoculation, the adults showed significantly greater lung weight changes than the young mice ($P < 0.01$). The lungs of infected young and adult mice were also subjected to histopathological analysis on days 1 to 5 after inoculation (Figure 3, A–H). On day 1 after inoculation, both young and adult mice had antigen-positive epithelial cells in the bronchi and alveoli. The antigen-positive cells in the alveoli were considered on the bases of morphology and immunohistochemistry to be mainly type II pneumocytes (Figure 3, A and E; see Supplemental Figure S1 at *http://ajp.amjpathol.org*). On day 2 after inoculation, antigen-positive atrophic and necrotic cells were seen in the alveolar area of both mice (Figure 3B). In addition, antigen-positive activated alveolar macrophages associated with inflammatory infiltrations were seen in the alveolar area of adult mice (Figure 3F). No antigen-positive cells were seen in the bronchi on day 2 after inoculation or afterward in either young or adult mice. On day 3 after inoculation, the young mice had diffuse inflammatory infiltrates consisting mainly of mononuclear cells (Figure 3, C and D), and virus antigen-positive cells were seen in the alveolar area. Activated macrophages, lymphocytes, and neutrophils were seen in the alveoli on days 4 and 5 after inoculation. In contrast, the adult mice evinced severe pulmonary edema, and congestion on day 3 after inoculation (Figure 3, G and H). In these mice, the main inflammatory cells around the adult blood vessels and alveolar area on days 3 to 5 after inoculation were neutrophils and activated macrophages. Fibrin deposition and hyaline membrane formation in the alveolar duct and alveoli were also observed (Figure 3H), and microhemorrhages was seen in the alveolar area. The adult mice also had high virus titers in the lung and maxilla (including nasal cavity) and their fluid (Figure 2, D and E). After the infection, virus continued to be isolated from the cervical lymph nodes, spleen, liver, and kidneys of adult mice after day 2 after inoculation whereas virus could no longer be isolated from any young mouse tissue (apart from the lung) after this time point (Table 1).

Different Immune Responses to SARS-CoV in Young and Adult Mice

To analyze the immune responses of young and adult mice after infection with F-musX-VeroE6, we examined their peripheral blood white blood cell counts (Figure 4), and measured the levels of 20 different chemokines and cytokine levels in their plasma and lung homogenates (Figures 5 and 6). Before infection (day 0), the adult mice had significantly lower white blood cells counts, especially with regard to lymphocytes (including $CD4^+$ and $CD8\beta^+$ T cells), than the

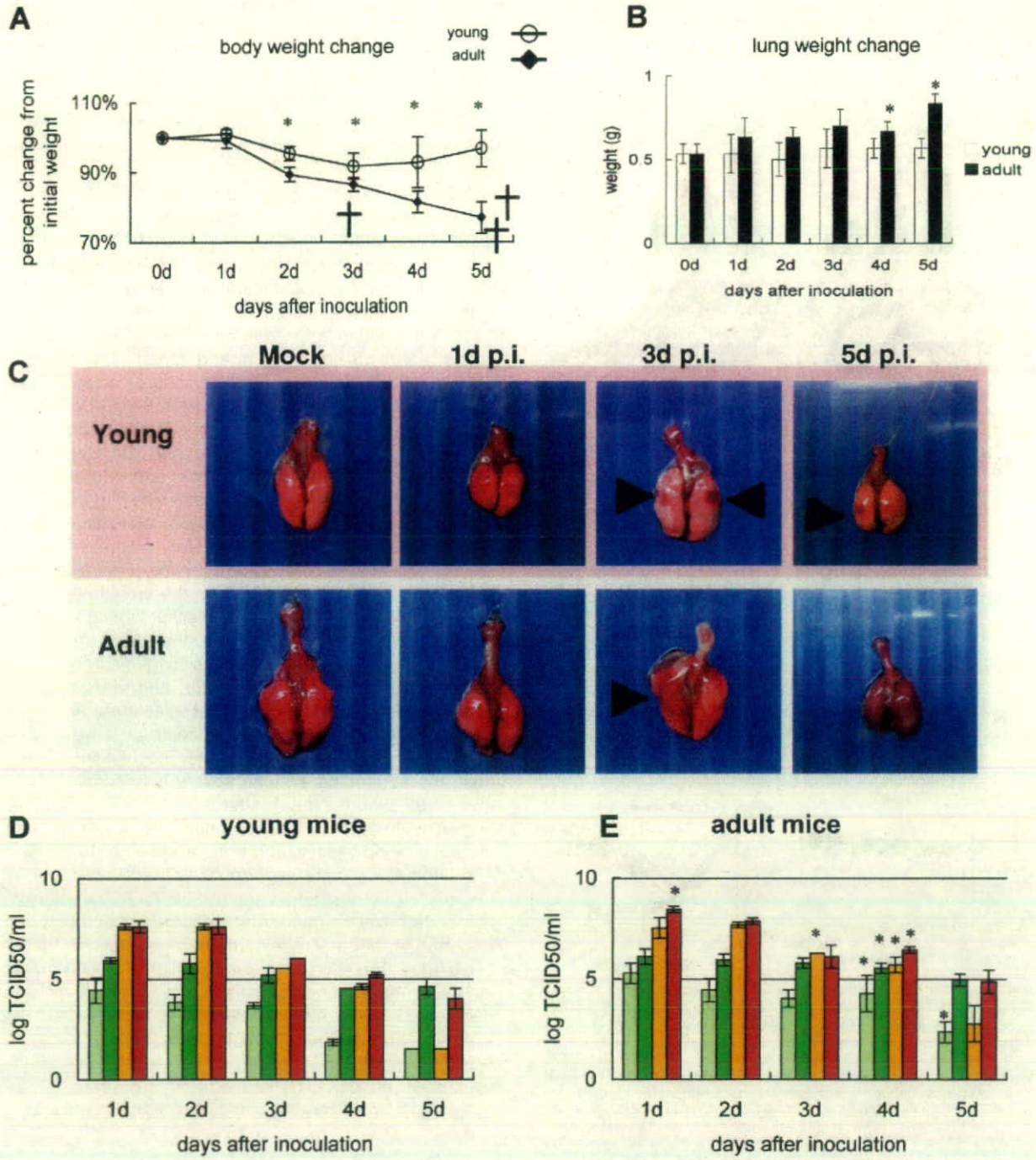

Figure 2. The pathophysiology induced by mouse-passaged SARS-CoV differs between young and adult mice. F-musX-VeroE6-infected young and adult mice were examined at the same time points after inoculation. **Asterisks** indicate statistically significant differences between young and adult mice ($P < 0.05$). **A:** Mean change in body weight (expressed as a percentage of the body weight on day 0) ($n = 6$ per group). Three (50%) of the adult mice became moribund and died (crosses) by day 5 after inoculation. **B:** To assess the lungs for pulmonary edema, the lungs were weighed after mice were sacrificed on days 1 to 5 after inoculation by exsanguination under anesthesia ($n = 3$ per group). **C:** Lungs from virus- and mock-infected young and adult mice obtained at the indicated time points after inoculation. **Arrowheads** indicate focal congestion. On day 5 after inoculation, a moribund adult mouse had dark red congested lungs. **D** and **E:** Virus titers in the nasal (pale green bar) and lung (yellow bar) wash fluids and homogenates of the maxilla (including nasal cavity, green bar) and lung (orange bar) on days 1 to 5 after inoculation ($n = 3$ per group). The detection limit was $10^{1.5}$ $TCID_{50}$/g of tissue.

young mice (Figure 4). After infection, the neutrophil counts in the adult mice increased; however, this change was not observed in the young mice. In young mice, relative to counts on day 0, lymphocyte counts decreased significantly ($P < 0.05$) on days 2, 3, and 4 after inoculation but then recovered, $CD8\beta^+$ T-cell counts decreased significantly on day 2 and then recovered, and $CD4^+$ T-cell counts decreased slightly and then showed a significant

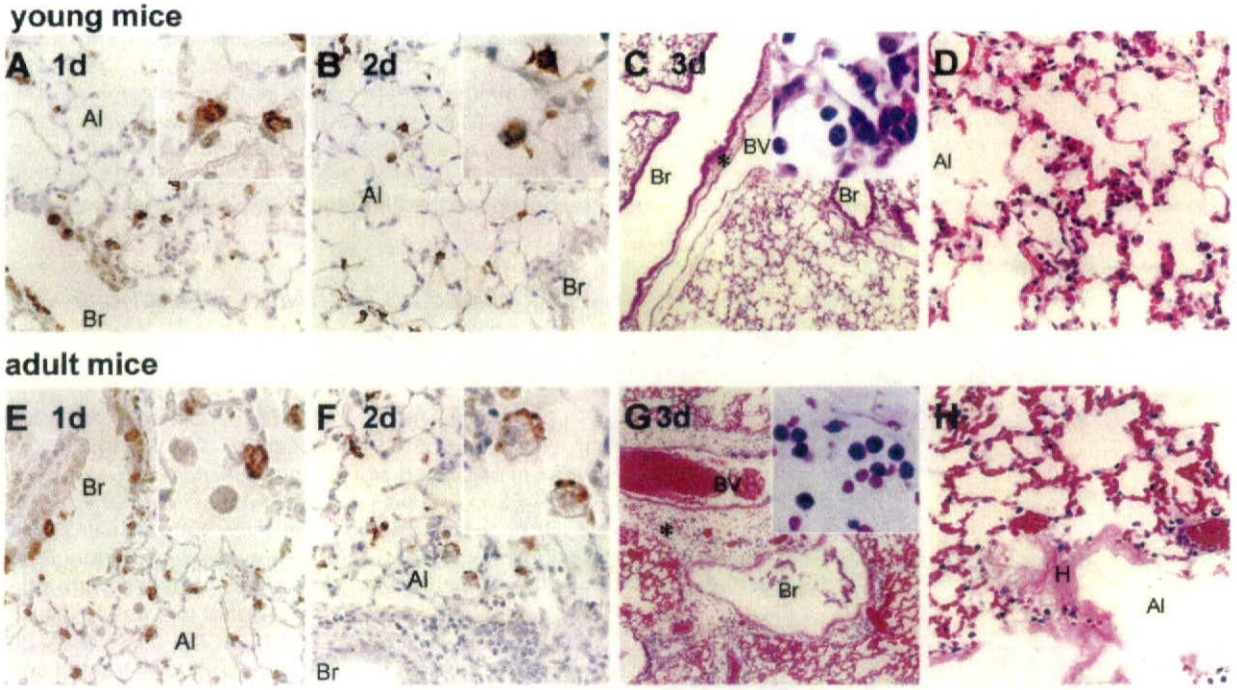

Figure 3. Histopathological findings in the lungs of young (**A–D**) and adult (**E–H**) mice on days 1 (**A**, **E**), 2 (**B**, **F**), and 3 (**C**, **D**, **G**, **H**) after inoculation. Br, bronchi; Al, alveoli; BV, blood vessel; H, hyaline membrane. The results in each panel are representative of at least three mice for each panel. Immunohistochemical staining with anti-SARS-CoV-specific antibody revealed virus antigen-positive cells in pulmonary epithelial cells of the bronchi and alveolar area, and type II pneumocytes (**inset**) in both young and adult mice on day 1 after inoculation (**A**, **E**). On day 2 after inoculation, atrophic cells in the alveolar area of young mice were positive for virus antigen (**B**, **inset**). In adult mice at the same time point activated alveolar macrophages presented in the alveolar space were also positive for virus antigen (**F**, **inset**). On day 3 after inoculation, the young mice showed slight inflammatory mononuclear cell infiltration in the alveolar area (**C**, **inset**; and **D**) but the adult mice exhibited massive pulmonary edema and inflammatory polynuclear leukocyte infiltration around blood vessels (**G**, **inset**). **H:** They also showed hyaline membrane formation in the alveolar duct.

increase on day 5. In contrast, although the lymphocyte counts of adult mice also dropped and were significantly lower than day 0 counts on days 3 and 4, they did not evidence an improvement on day 5 after inoculation. Moreover, the $CD8\beta^+$ T- and $CD4^+$ T-cell counts of the adult mice also showed significant drops on days 1, 3, and 4 after inoculation ($P < 0.05$) but had recovered poorly on day 5 after inoculation, unlike the counts in young mice. With regard to the $PanNK^+$ cells counts, both the young and adult mice showed a marked drop on day 1 after inoculation that was followed by a brief recovery and then another loss on day 4 after inoculation cell count loss at day 1 and 5 days after inoculation compared with 0 days after inoculation in adult mice ($P < 0.05$).

With regard to the cytokine responses of the mice, the lung homogenates of adult mice on day 1 after inoculation had significantly higher levels of monocyte-related chemokines [ie, MCP-1, macrophage inflammatory protein 1 (MIP-1), and IFN-γ-inducible protein 10 (IP-10)] than those from young mice (Figure 5). In contrast, on day 2 after inoculation, the lung homogenates of young mice exhibited elevated levels of these three cytokines as well as KC, monokine induced by IFN-γ (MIG), and vascular endothelial growth factor (VEGF) (Figure 5). Compared to young mice, the lung homogenates of adult mice on day 1 after inoculation also had higher levels of IL-1α, IL-1β, and TNF-α, and on day 3 after inoculation, higher levels of IL-6 were

Table 1. Virus Isolation from Different Tissues of F-musX-VeroE6-Infected BALB/c Mice at Various Time Points after Inoculation (n = 3 per Time Point)

	Young mice (4-week-old BALB/c)					Adult mice (6-month-old BALB/c)				
Days after inoculation	Lung	Cervical L/N	Spleen	Liver	Kidney	Lung	Cervical L/N	Spleen	Liver	Kidney
0 days	0*	0	0	0	0	0	0	0	0	0
1 day	3	3	3	1	0	3	3	3	3	0
2 days	3	3	2	2	0	3	3	2	2	1
3 days	3	0	0	0	0	3	2	1	1	1
4 days	3	0	0	0	0	3	2	0	0	0
5 days	3	0	0	0	0	3	0	1	0	0

*Number of virus isolation-positive animals.
L/N, lymph node.

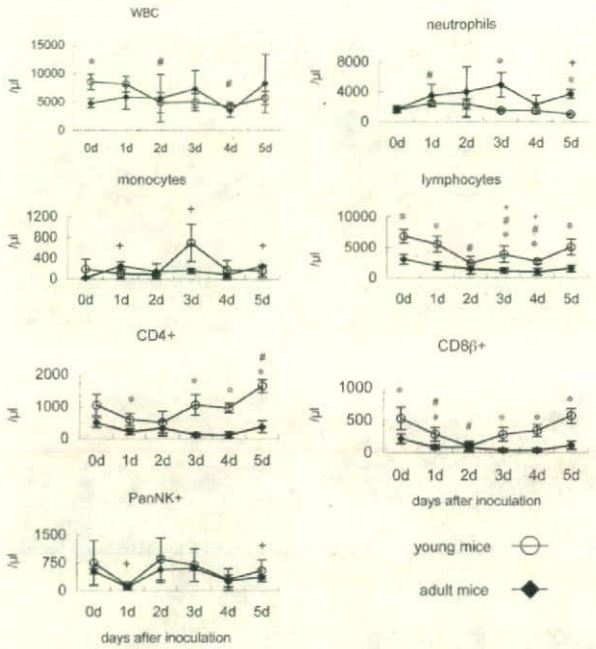

Figure 4. White blood cell (WBC) counts in young and adult mice throughout time after inoculation. Shown are total WBC, neutrophil, monocyte, lymphocyte, CD4-positive cell, CD8β-positive cell, and NK cell counts in the peripheral blood of young and adult mice after intranasal inoculation with mouse-passaged SARS-CoV ($n = 3$). $^{*}P < 0.05$ indicate statistically significant differences between young and adult mice at the same time point. $^{*}P < 0.05$ and $^{+}P < 0.05$ indicate statistically significant differences within groups relative to day 0 in young or adult mice, respectively.

observed (Figure 6). In contrast, the lung homogenates of young mice had significantly higher levels of IFN-γ (on day 2 after inoculation), IL-2 (on days 2 to 5 after inoculation), IL-10 (on days 0, and 2 to 5 after inoculation), and IL-13 (on days 0 to 2, and 4 and 5 after inoculation). Notably, the lung homogenates of preinfected adult mice (day 0) had higher IL-4 and lower IL-10 and IL-13 levels than young murine lungs. These observations indicate that the patterns of cytokine/chemokines responses are different between young and adult mice after SARS-CoV infection. Adult mice showed early and acutely excessive proinflammatory responses in the lung after SARS-CoV infection.

Effect of Injecting Anti-TNF-α Antibody or IFN-γ on the Pathogenesis of Mouse-Adapted SARS-CoV in Adult Mice

To determine whether the TNF-α response of the adult mice and the IFN-γ produced by the young but not adult mice played significant roles in the development of SARS-like illness by the F-musX-VeroE6-infected adult mice, we treated adult mice with an anti-TNF-α antibody or IFN-γ 3 hours after infection (Figure 7, A and B). Although the intravenous injection with anti-TNF-α antibody delayed the onset of this weight loss in the infected adult mice, as well as the onset of respiratory illness, both the anti-TNF-α antibody-treated and control adult mice showed significant body weight loss up until 6 days after inoculation and there were no significant differences in mortality rates between treated and control adult mice (treated adult mice: 62.5%, 50% mortality rate; control adult mice: 37.5%, 37.5% mortality rate in two separate experiments) (Figure 7A). In contrast, the IFN-γ-treated mice rapidly recovered from the illness as evidenced by their body weight loss and severe acute respiratory symptoms and all animals survived after onset 3 days after inoculation (Figure 7B). In contrast, 50% of the control adult mice died.

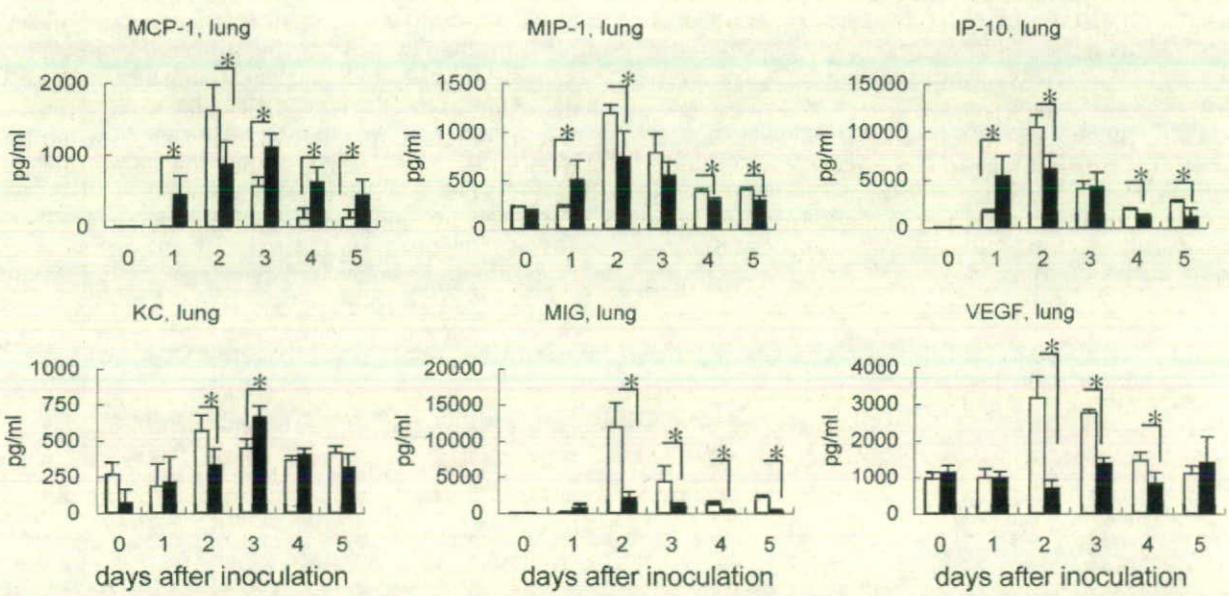

Figure 5. Chemokine protein levels in the lungs of young (white bar) and adult (black bar) mice throughout time after inoculation ($n = 3$ per group). **Asterisks** indicate statistically significant higher or lower chemokine levels in adult mice ($P < 0.05$) compared to young BALB/c mice. Adult mice showed earlier induction of MCP-1, MIP-1, and IP-10 in the lungs than young mice but these three chemokines and MIG and VEGF were at significantly higher levels in the lungs of young mice on day 2 after inoculation.

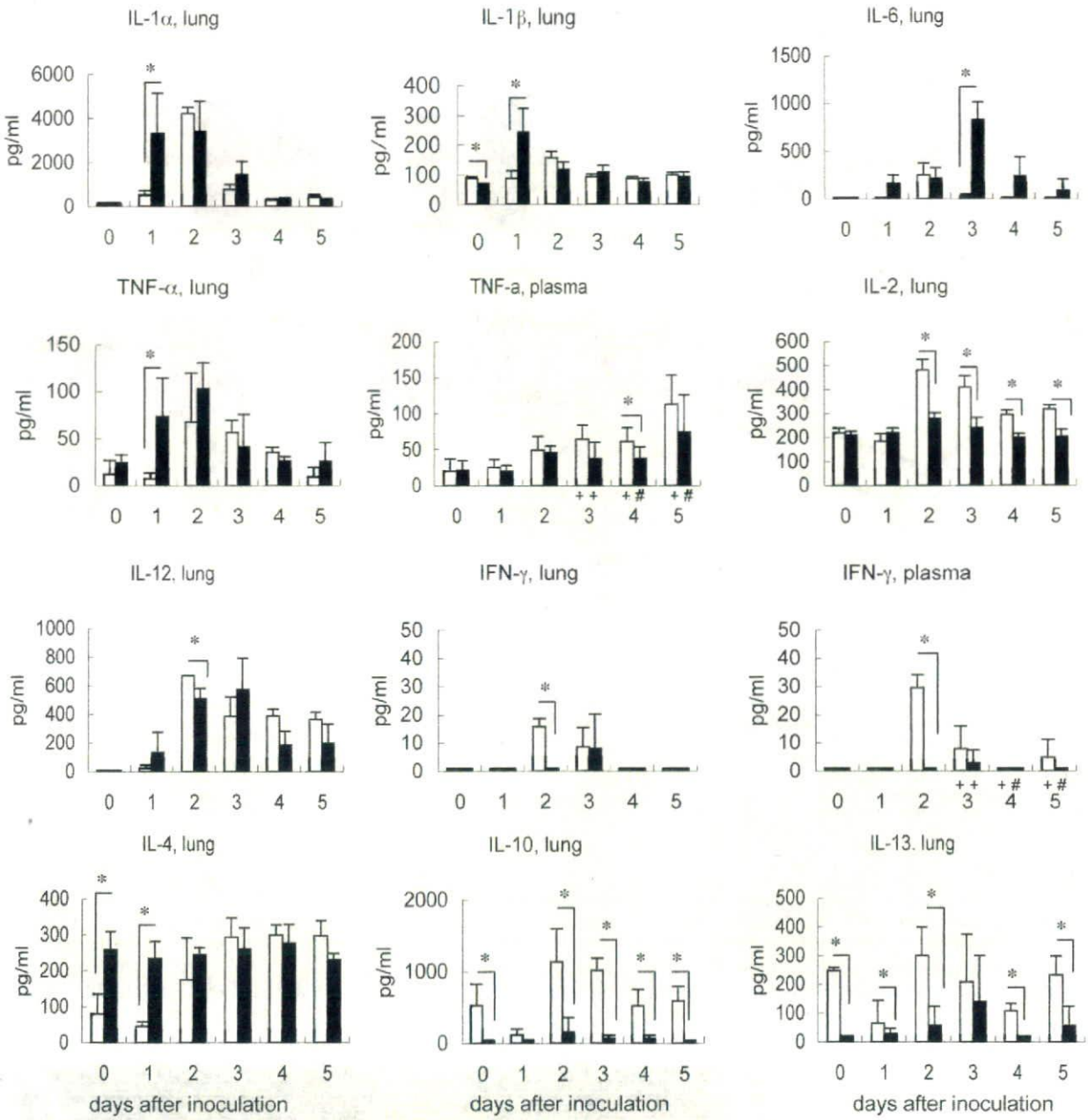

Figure 6. Cytokine protein levels in lungs and plasma throughout time after inoculation ($n = 3$ per group; $^{+}n = 6$; $^{*}n = 4$). **Asterisks** indicate statistically significant higher or lower cytokine levels in adult mice ($P < 0.05$) compared to in young mice. The adult mice had significantly higher levels of IL-1α, IL-1β, IL-6, TNF-α, and IL-4 whereas the young mice had significantly higher levels of IL-2, IL-12, IFN-γ, IL-10, and IL-13.

To determine whether the protective effect of IFN-γ treatment is attributable to suppression of viral replication, the virus titers on the day 3 after inoculation of nasal washes, maxilla homogenates, lung washes, and lung homogenates of IFN-γ-treated and PBS-treated adult mice after the infection were compared. However, the two groups did not differ significantly in terms of virus titers in the respiratory tracts (Figure 7C). The IFN-γ-treated mice showed much milder histopathological changes than the untreated mice because only very mild edema with slight mononuclear cell infiltration was observed around the blood vessels after the infection (Figure 7D). In contrast, the PBS-treated mice exhibited severe edema and infiltration of inflammatory cells, mainly neutrophils, around blood vessels (Figure 7E). By examining Evans blue dye extravasation, we found the IFN-γ-treated mice also had lower blood vessel permeability than the PBS-treated mice (Figure 8, A–G). Together, these results suggest that IFN-γ treatment 3 hours after inoculation protected the mice from severe SARS-CoV-induced pulmonary edema that was responsible for the death of the untreated adult mice.

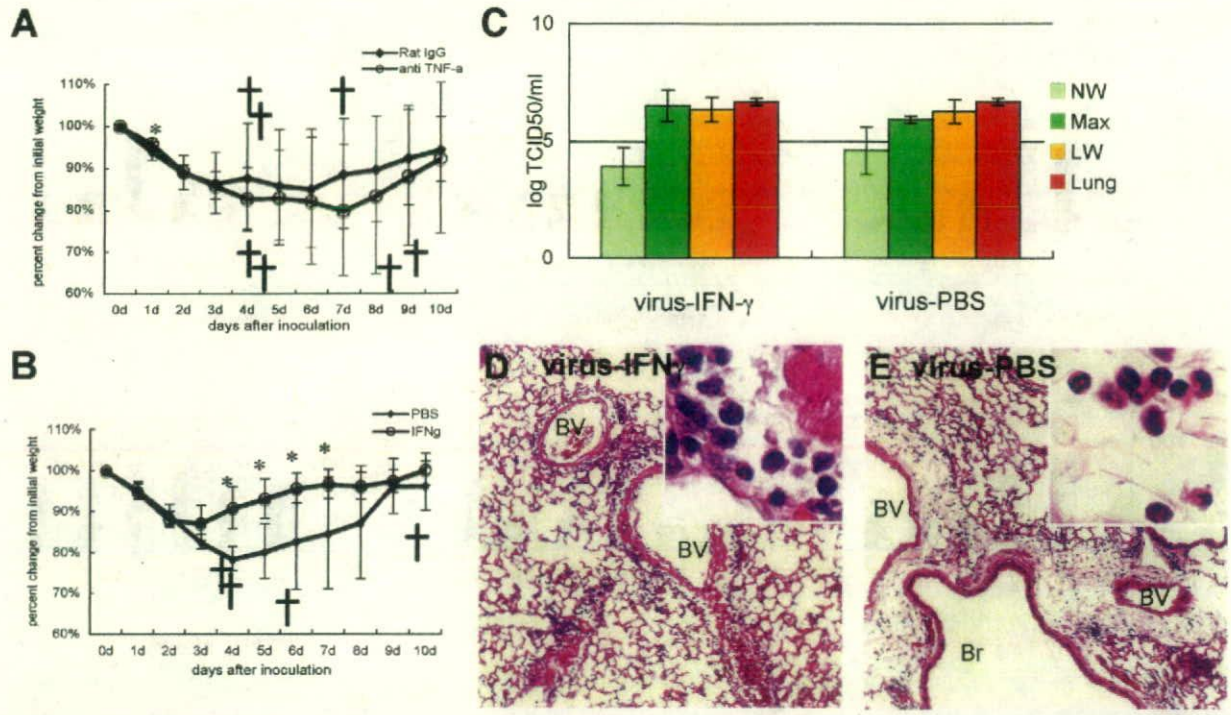

Figure 7. Effect of anti-TNF-α antibody or IFN-γ injections of infected adult mice on body weight change throughout time after inoculation. Adult mice were infected with F-musX-VeroE6 by intranasal inoculation and injected intravenously with anti-TNF-α antibody or intraperitoneally with IFN-γ 3 hours after inoculation. Mean percentages of body weight change of the animals were determined for 10 days after inoculation. **Crosses** indicate dead mice. **Asterisks** indicate statistically significant differences in weight loss ($P < 0.05$) compared to control animals. The results shown in each panel are representative of at least two independent experiments for each panel ($n = 5$ to 8 per group). **A:** Effect of anti-TNF-α antibody ($n = 8$ per group). The control group was injected intravenously with rat IgG. **B:** Effect of IFN-γ ($n = 8$ per group). The control group was injected with PBS intraperitoneally. **C:** Virus titers in the nasal (pale green bar) and lung (yellow bar) wash fluids and homogenates of the maxilla (including nasal cavity, green bar) and lung (orange bar) on days 3 after inoculation of PBS- and IFN-γ-treated adult mice ($n = 3$ per group). The detection limit was $10^{1.5}$ $TCID_{50}$/g of tissue. **D** and **E:** Lung histopathology in IFN-γ- and PBS-treated adult mice, respectively. BV, blood vessel; Br, bronchi. Mononuclear cell infiltration was seen in the alveolar area and around blood vessels in the lungs of the IFN-γ-injected mice (**D**, **inset**). In contrast, the lungs of PBS-injected mice exhibited polynuclear leukocyte infiltration around edematous blood vessels (**E**, **inset**).

Discussion

To understand better the pathogenesis of SARS after SARS-CoV infection, we developed a useful experimental mouse model of SARS. When the Frankfurt 1 isolate of SARS-CoV was serially passaged *in vivo* in young BALB/c mice, the passaged virus (F-musX-VeroE6) exhibited increased infectivity in the murine lung. F-musX-VeroE6 was also able to induce severe SARS-like illness in adult (6-month-old) BALB/c mice and several animals died of severe pulmonary edema and acute alveolar damage. However, young (4-week-old) mice were relatively resistant to F-musX-VeroE6 and did not evince any obvious respiratory illness. When the immune responses of in-

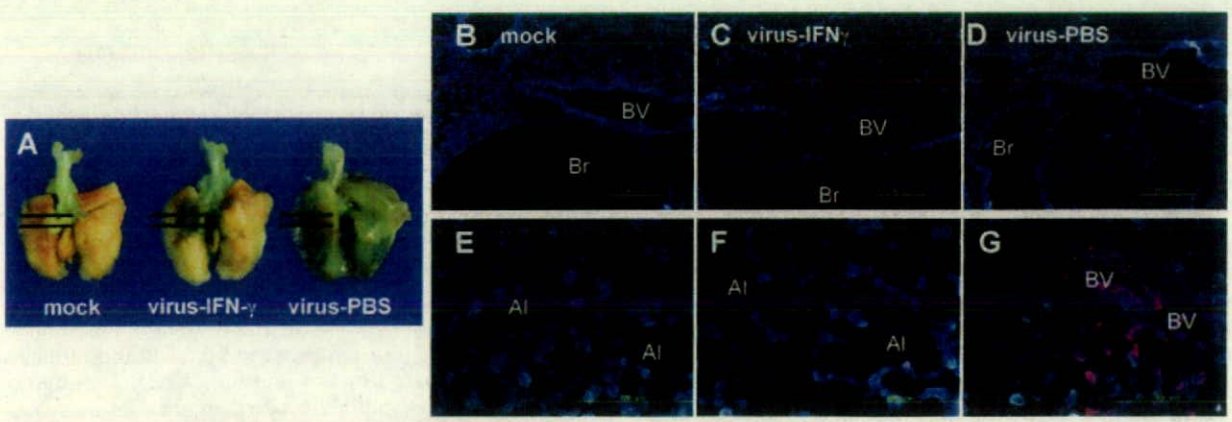

Figure 8. A–G: IFN-γ treatment protects mice from infection-induced blood vessel hyperpermeability in the lung. Virus-infected adult mice ($n = 3$) were injected intraperitoneally with IFN-γ or PBS and the effect of these treatments on lung blood vessel permeability was determined by using Evans blue dye extravasation. **A:** Blue discoloration of the lung tissue of IFN-γ- and PBS-treated mice 3 days after inoculation. The black lines indicate the areas examined in more detail in **B–G**. **B–G:** The deposition of Evans blue dye in lung tissue (pink) was examined in frozen sections of the formalin-fixed tissue by using a fluorescence microscope. Scale bars: 200 μm (**B–D**); 100 μm (**E–G**).